Journal of Photochemistry & Photobiology A: Chemistry 386 (2020) 112125

Contents lists available at ScienceDirect

Journal of Photochemistry & Photobiology A: Chemistry

journal homepage: www.elsevier.com/locate/jphotochem

Indolizine-based chromophores with octatetraene π-bridge and tricyanofurane acceptor: Synthesis, photophysical, electrochemical and electro-optic properties

Alexey A. Kalinin[a,*], Guzel M. Fazleeva[a], Timur I. Burganov[a], Liliya N. Islamova[a], Yulia B. Dudkina[a], Alfira A. Kadyrova[a], Tatyana A. Vakhonina[a], Ayrat R. Khamatgalimov[a], Anvar S. Mukhtarov[a], Valeriy V. Bazarov[b], Sergey A. Katsyuba[a], Yulia H. Budnikova[a], Marina Yu. Balakina[a]

[a] Arbuzov Institute of Organic and Physical Chemistry, FRC Kazan Scientific Center of RAS, Arbuzov Str. 8, 420088 Kazan, Russia
[b] Zavoisky Physical-Technical Institute, FRC Kazan Scientific Center of RAS, Sibirsky tract 10/7, 420029, Kazan, Russia

ARTICLE INFO

Keywords:
Indolizine chromophores
Synthesis
Solvatochromic behavior
Cyanine limit
Voltammetry
EO coefficient

ABSTRACT

Two isomeric indolizine-based chromophores **(MPI-1)-OT-TCF** and **(MPI-3)-OT-TCF** with octatetraene π-bridge and tricyanofuran acceptor moieties have been synthesized and systematically investigated. Chromophores exist as a mixture of *E*- and *Z*-isomers in low-polar dioxane and chloroform solutions, while in polar solvents only one isomer is observed. The chromophores show excellent thermal stability with T_d > 260 °C (DSC) and small energy gap between the frontier orbitals (about 0.8–0.9 eV) established by DPV method. The chromophores exhibit absorption in the visible and near IR region. Solvatochromic shifts amounting to ca. 100 nm when passing from dioxane to DMSO solutions are accompanied by appearance of an additional narrow intensive absorption band at ca. 915–950 nm resulting from the cross of cyanine limit. For the first time electro-optic activity of composite materials doped by indolizine based chromophores have been investigated; EO coefficient of poled **(MPI-3)-OT-TCF/PMMA** film afforded value of 29 pm/V at 10 wt% load.

1. Introduction

D-π-A chromophores with heterocyclic donor moieties exhibiting absorption/emission in the visible and near IR region are widely used in various fields of photonics and organic electronics. Composite materials doped with thiophene- and pyrrole-based chromophores [1] as well as fused heterocyclic indolylidenmethylene- [2,3], phenothiazine- [4], phenoxazine- [4] and julolidine-based ones [5–9], containing π-expanded bridge, strong tricyanofuran (TCF) acceptor moiety [10] and various bulky groups to reduce chromophores aggregation show significant nonlinear optical (NLO) effect to give electro-optic (EO) coefficient, r_{33}, of 23–230 pm/V. In this case, a suitable isolating groups (including those of dendrimer type) or bulky groups with opposite effect, enhancing non-centrosymmetric chromophore ordering through nonvalent interactions, lead to a further increase in the EO activity of materials [11–13]. Dye-sensitized solar cells (DSSC) based on indoline [14–16], tetrahydroquinoline [17], carbazole [18], coumarin [19] and cyclopentadithiophene [20] dyes achieved the good energy conversion and incident photon to current conversion efficiency. One of the challenges emphasized by researchers in the field of design of NLO materials as well as dye-sensitized solar cells is the increase in the strength of the chromophores donor unit. To enhance the electronic donation ability of the aniline donor of the chromophores, additional heteroatoms were introduced into this moiety, usually in the *orto*-position to the π-bridge [21–24]. Such modification produced both an increase in the values of the first hyperpolarizability - molecular NLO characteristics - and the macroscopic NLO/EO response of materials. The second approach consists in the use of nitrogen heterocyclic donors more planar than dialkyl/diaryl aniline ones. For example, changing the dialkyl aniline [25,26] donor for heterocyclic julolidine one [5,25] in

* Corresponding author.
E-mail addresses: kalesha007@mail.ru (A.A. Kalinin), Fazleeva_GM@mail.ru (G.M. Fazleeva), timk90@mail.ru (T.I. Burganov), nailisllil1989@mail.ru (L.N. Islamova), dudkinayu@iopc.ru (Y.B. Dudkina), Kadirovaalfira@mail.ru (A.A. Kadyrova), tanyavakhonina@yandex.ru (T.A. Vakhonina), ayrat_kh@iopc.ru (A.R. Khamatgalimov), mukhtarovy@yandex.ru (A.S. Mukhtarov), bazarov@kfti.knc.ru (V.V. Bazarov), skatsyuba@yahoo.com (S.A. Katsyuba), yulia@iopc.ru (Y.H. Budnikova), mbalakina@yandex.ru (M.Y. Balakina).

https://doi.org/10.1016/j.jphotochem.2019.112125
Received 16 August 2019; Received in revised form 20 September 2019; Accepted 27 September 2019
Available online 30 September 2019
1010-6030/ © 2019 Elsevier B.V. All rights reserved.

chromophore results in red shift of the lowest-energy absorption band, which indicates a greater donor strength of julolidine moiety. A lot of julolidine-based D-π-A chromophores exhibit outstanding NLO activity in the guest-host materials [5–9]. Strategy for increasing the electron-donating strength of common nitrogen-based donors including planarization of nitrogen substituents and the use of heteroaromatic rings with bridge nitrogen atom has been applied: for example, application of chromophore with a planar indolizine moiety for DSSCs allowed increasing device efficiencies up to 8% [27–29]. The bridging nitrogen atom in the indolizine contributes to the localization of a significant π-electron density at its C1/C3 carbon atoms and at the heterocycle as a whole [30], thus promoting the high first hyperpolarizability of indolizine-based chromophores with strong acceptor moieties and extensive π-bridge [30,31]. Indolizine dyes display strong NIR absorption and emissions and a large Stokes shift [32–34]. Alongside with application of indolizine derivatives in DSSC devices, luminescent materials [35,36] and macrocyclic compounds [37,38] exhibiting redox switchable binding of some cations have been fabricated [39,40]. Here we present the synthesis and the study of photophysical, thermal and electrochemical properties of chromophores with isomeric indolizine donor and TCF acceptor moieties, coupled by π-extended octatetraene bridge. For the first time EO activity of composite polymer materials doped with indolizine-based chromophores is studied.

2. Experimental section

2.1. Materials and instrumentation

Acetophenone, propiophenone, 2-ethylpyridine, 2-picoline, 3-hydroxy-3-methyl-2-butanone and malononitrile were purchased from Acros or Aldrich. Organic solvents used were purified and dried according to standard methods. The melting points presented in Section 2.2 were determined on a Boetius hot-stage apparatus. Infrared (IR) spectra were recorded on the Bruker Vector-22 FT IR spectrometer. NMR experiments were performed with Bruker AVANCE-600, AVANCE-500, and AVANCE-400 (600, 500 and 400 MHz for ^{1}H NMR, 150, 125 and 100 MHz for ^{13}C NMR) spectrometers. Chemical shifts (δ in ppm) are referenced to the solvents. The mass spectra were obtained on Bruker UltraFlex III MALDI TOF/TOF instrument with *p*-nitroaniline as a matrix. UV–vis spectra were recorded at room temperature on a Perkin-Elmer Lambda 35 spectrometer using 10 mm quartz cells. Spectra were registered with a scan speed of 480 nm/min, using a spectral width of 1 nm. All samples were prepared in solution with the concentrations of ca $\sim 10^{-5}$ mol/L. The thermal stabilities of chromophores **(MPI-1)-OT-TCF** and **(MPI-3)-OT-TCF** were investigated by simultaneous thermal analysis (thermogravimetry/differential scanning calorimetry - TG/DSC) using NETZSCH (Selb, Germany) STA449 F3 instrument. Approximately 2.7–3.8 mg samples were placed in an Al crucible with a pre-hole on the lid and heated from 30 to 600 °C. The same empty crucible was used as the reference sample. High-purity argon was used with a gas flow rate of 50 mL/min. TG/DSC measurements were performed at the heating rates of 10 K/min.

2.2. Synthesis methodology

2.2.1. (E)-5,5-Dimethyl-3-(2-(3(1)-methyl-2-phenylindolizin-1(3)-yl)vinyl)cyclohex-2-en-1-ones (5a,b)

Sodium (0.40 g, 0.017 mmol) was dissolved in ethanol (10 mL) then 3(1)-methyl-2-phenylindilizine-1(3)-carbaldehede (4.00 g, 0.017 mmol) and isophorone (2.60 g, 0.19 mmol) were added. Reaction mixture was refluxed for 18 h, cooled to room temperature and ethanol was evaporated. The residue was purified by silica-gel column chromatography (eluent: methylene chloride) to give a color product and unreacted 3(1)-methyl-2-phenylindilizine-1(3)-carbaldehyde (2.60 g (2.90 g)) was returned.

2.2.1.1. (E)-5,5-Dimethyl-3-(2-(3-methyl-2-phenylindolizin-1-yl)vinyl)cyclohex-2-en-1-one (5a).

Yield: 0.99 g (16%). Dark red viscous oil. R_f = 0.15 (hexane:ethyl acetate = 5:1) ^{1}H NMR (400 MHz, $CDCl_3$): δ 7.78 (d, *J* = 6.7 Hz, 1H, H-5 indolizine), 7.76 (d, *J* = 8.8 Hz, 1H, H-8 indolizine), 7.50-7.45 (m, 2H, *m*-Ph), 7.43-7.38 (m, 1H, *p*-Ph), 7.37-7.33 (m, 2H, *o*-Ph), 7.19 (d, *J* = 16.2 Hz, 1H, ethene), 6.94 (ddd, *J* = 8.8, 6.6, 1.1 Hz, 1H, H-7 indolizine), 6.73 (ddd, *J* = 6.7, 6.6, 1.1 Hz, 1H, H-6 indolizine), 6.43 (d, *J* = 16.2 Hz, 1H, ethene), 5.77 (s, 1H, −CH(CO)-), 2.37 (s, 3H, CH_3), 2.36 (s, 2H, CH_2), 2.24 (s, 2H, CH_2), 1.06 (s, 6H, CH_3). ^{13}C NMR (100 MHz, $CDCl_3$): δ 200.0, 156.9, 135.0, 131.7, 130.7, 128.4, 128.0, 127.9, 127.2, 124.5, 123.6, 122.7, 119.8, 119.3, 118.0, 112.0, 108.7, 51.4, 38.8, 33.2, 28.6, 9.9. IR (λ_{max}, cm^{-1}, KBr): 3458 (CH), 2955 (CH), 1651 (C = O), 1596 (C = C). MALDI-TOF: 356 $[M+H]^+$.

2.2.1.2. (E)-5,5-Dimethyl-3-(2-(3-methyl-2-phenylindolizin-1-yl)vinyl)cyclohex-2-en-1-one (5b).

Yield: 1.03 g (17%). Dark red viscous oil. R_f = 0.27 (hexane:ethyl acetate = 5:1). ^{1}H NMR (600 MHz, $CDCl_3$): δ 8.25 (d, *J* = 6.6 Hz, 1H, H-5 indolizine), 7.46 (dd, *J* = 7.7, 7.3 Hz, 2H, *m*-Ph), 7.43-7.37 (m, 2H, *p*-Ph, H-8 indolizine), 7.33 (d, *J* = 7.7 Hz, 2H, *o*-Ph), 7.12 (d, *J* = 16.2 Hz, 1H, ethene), 6.86-6.79 (m, 1H, H-7 indolizine), 6.68 (ddd, *J* = 6.7, 6.5 Hz, 1H, H-6 indolizine), 6.39 (d, *J* = 16.2 Hz, 1H, ethene), 5.75 (s, 1H, −CH(CO)-), 2.33 (s, 2H, CH_2), 2.23 (s, 2H, CH_2), 2.20 (s, 3H, CH_3), 1.05 (s, 6H, CH_3). ^{13}C NMR (150 MHz, $CDCl_3$): δ 199.6, 156.1, 135.2, 133.7, 132.6, 130.4, 128.4, 127.3, 124.3, 123.6, 123.4, 121.8, 118.7, 118.5, 117.8, 112.0, 110.5, 51.3, 38.7, 33.1, 28.5, 8.9. IR (λ_{max}, cm^{-1}, KBr): 3438 (CH), 2956 (CH), 1643 (C = O), 1593 (C = C), 1573 (C = C). MALDI-TOF: 356 $[M+H]^+$.

2.2.2. (E,Z)-2-(5,5-dimethyl-3-((E)-2-(3(1)-methyl-2-phenylindolizin-1(3)-yl)vinyl)cyclohex-2-en-1-ylidene)acetonitriles (6a,b)

To the stirred mixture of NaH (0.12 g, 5.0 mmol) and dry THF (3 mL) diethyl cyanomethyphosphonate (0.87 g, 5.0 mmol) in dry THF (1 mL) was added dropwise by syringe at 0 °C. When the solution became transparent, indolizine **5** (0.70 g, 2.0 mmol) solution in dry THF (10 mL) was added. The mixture was refluxed for 18 h, and then after removal of the THF, the residue was purified by column chromatography (eluent: hexane/methylene chloride = 3:1→1:1).

2.2.2.1. (E,Z)-2-(5,5-dimethyl-3-((E)-2-(3-methyl-2-phenylindolizin-1-yl)vinyl)cyclohex-2-en-1-ylidene)acetonitrile (6a).

Yield: 0.63 g (84%). Dark red powder, mp 74–75 °C. R_f = 0.18 (hexane:ethyl acetate = 20:1). ^{1}H NMR (400 MHz, acetone-d_6): δ 7.98 (d, *J* = 7.0 Hz, 1H, H-5 indolizine), 7.97 (d, *J* = 7.0 Hz, 1.4H, H-5 indolizine), 7.93 (d, *J* = 9.0 Hz, 1H, H-8 indolizine), 7.85 (d, *J* = 9.0 Hz, 1.4H, H-8 indolizine), 7.53-7.47 (m, 4.8H, *m*-Ph), 7.43-7.36 (m, 7.2H, *o,p*-Ph), 7.10 (d, *J* = 16.3 Hz, 1H, ethene), 7.07 (d, *J* = 16.3 Hz, 1.4H, ethene), 6.97-6.90 (m, 2.4H, H-7 indolizine), 6.80-6.74 (m, 2.4H, H-6 indolizine), 6.66 (d, *J* = 16.3 Hz, 1H, ethene), 6.48 (d, *J* = 16.3 Hz, 1.4H, ethene), 6.41 (s, 1H, -CH=C(R)CH(CN)-), 6.06 (s, 1.4H, -CH=C(R)CH(CN)-), 5.14 (s, 1.4H, =CH(CN)-), 5.00 (s, 1H, =CH(CN)-), 2.39-2.37 (br, 5.8H, CH_2, CH_3), 2.36 (s, 4.2H, CH_3), 2.26 (br, 4.8H, CH_2), 2.21 (br, 2H, CH_2), 0.98 (s, 8.4H, CH_3), 0.94 (s, 6H, CH_3). ^{13}C NMR (100 MHz, acetone-d_6): δ 158.9, 158.7, 147.8, 146.9, 136.3, 136.2, 131.75, 131.73, 131.61, 131.58, 129.1, 128.2, 128.0, 127.8, 126.3, 126.2, 126.17, 125.7, 124.1, 123.9, 121.6, 120.3, 120.2, 119.7, 119.5, 119.0, 118.8, 118.2, 112.52, 112.46, 109.62, 109.60, 91.7, 90.2, 45.0, 42.6, 39.1, 38.9, 31.6, 31.5, 28.3, 28.2, 9.94, 9.88. IR (λ_{max}, cm^{-1}, KBr): 3437 (CH), 2924 (CH), 2199 (C≡N), 1607 (C = C), 1572 (C = C). MALDI-TOF: 379 $[M+H]^+$.

2.2.2.2. (E,Z)-2-(5,5-dimethyl-3-((E)-2-(1-methyl-2-phenylindolizin-3-yl)vinyl)cyclohex-2-en-1-ylidene)acetonitrile (6b).

Yield: 0.58 g (77%). Dark red powder, mp 65–66 °C. R_f = 0.22 (hexane:ethyl acetate = 20:1). ^{1}H NMR (400 MHz, $CDCl_3$): δ 8.60 (d, *J* = 7.0 Hz, 1H, H-5 indolizine), 8.51 (d, *J* = 7.1 Hz, 1.5H, H-5 indolizine), 7.55-7.47 (m, 7.5H, *m*-Ph, H-8

indolizine), 7.46-7.36 (m, 7.5H, *o,p*-Ph), 7.15 (d, J = 16.3 Hz, 2.5H, ethene), 6.90-6.83 (m, 2.5H, H-7 indolizine), 6.78-6.71 (m, 2.5H, H-6 indolizine), 6.63 (d, J = 16.4 Hz, 1H, ethene), 6.44 (d, J = 16.4 Hz, 1.5H, ethene), 6.36 (s, 1H, –CH=C(R)CH(CN)-), 6.02 (s, 1.5H, -CH=C(R)CH(CN)-), 5.20 (s, 1.5H, =CH(CN)-), 5.06 (s, 1H, =CH (CN)-), 2.40 (s, 1.5H, CH_2), 2.39 (s, 1.5H, CH_2), 2.32 (s, 3H, CH_2), 2.31 (s, 2H, CH_2), 2.25 (s, 1H, CH_2), 2.24 (s, 1H, CH_2), 1.00 (s, 9H, CH_3), 0.96 (s, 6 H, CH_3). ^{13}C NMR (100 MHz, $CDCl_3$): δ 158.1, 157.8, 146.1, 145.5, 135.5, 135.3, 133.3, 133.0, 132.0, 131.4, 130.6, 130.5, 128.4, 128.3, 127.2, 127.1, 125.4, 125.1, 124.6, 123.7, 123.1, 122.5, 119.8, 119.1, 119.0, 118.9, 118.8, 118.0, 117.8, 117.78, 117.72, 117.65, 111.9, 111.7, 110.1, 109.8, 91.5, 90.0, 44.8, 42.1, 38.49, 38.46, 31.2, 31.0, 28.2, 28.1, 9.00, 8.97. IR (λ_{max}, cm^{-1}, KBr): 3050 (CH), 2917 (CH), 2198 (C≡N), 1608 (C = C), 1567 (C = C). MALDI-TOF: 379 $[M+H]^+$.

2.2.3. (E,Z)-2-(5,5-Dimethyl-3-((E)-2-(3(1)-methyl-2-phenylindolizin-1(3)-yl)vinyl)cyclohex-2-en-1-ylidene)acetaldehydes (**7a,b**)

To the stirred and cooled to −78 °C solution of indolizine **6** (0.37 g, 1 mmol) in dry toluene (8 mL), diisobutylaluminium hydride (1.3 mL, 1.56 mmol) was added dropwise by syringe, then the mixture was stirred for 2 h at −78 °C and for 1 h at room temperature. Saturated aqueous NH_4Cl solution (5 mL) was added to quench the reaction, and mixture was stirred for 20 min at room temperature. Organic layer was separated and washed with water. Toluene was evaporated and the residue was purified by column chromatography (eluent: methylene chloride).

2.2.3.1. (E,Z)-2-(5,5-Dimethyl-3-((E)-2-(3-methyl-2-phenylindolizin-1-yl) vinyl)cyclohex-2-en-1-ylidene)acetaldehyde (**7a**).

Yield: 0.22 g (58%). Dark red powder, mp 75–77 °C. R_f = 0.33 (hexane:ethyl acetate = 10:3). ^{1}H NMR (600 MHz, acetone-d_6): δ 10.15 (d, J = 8.0 Hz, 1H, CHO), 10.02 (d, J = 8.2 Hz, 2.5H, CHO), 7.98 (d, J = 6.8 Hz, 1H, H-5 indolizine), 7.97 (d, J = 6.8 Hz, 2.5H, H-5 indolizine), 7.89 (d, J = 9.0 Hz, 1H, H-8 indolizine), 7.87 (d, J = 9.0 Hz, 2.5H, H-8 indolizine), 7.53-7.48 (m, 7H, *m*-Ph), 7.43-7.39 (m, 3.5H, *p*-Ph), 7.39-7.36 (m, 7H, *o*-Ph), 7.09 (d, J = 16.3 Hz, 1H, ethene), 7.14 (s, 1H, -CH=C(R)CH(CHO)-), 7.08 (d, J = 16.3 Hz, 3.5H, ethene), 6.94 (dd, J = 9.0, 6.7 Hz, 3.5H, H-7 indolizine), 6.76 (dd, J = 6.8, 6.7 Hz, 3.5H, H-6 indolizine), 6.69 (d, J = 16.3 Hz, 1H, ethene), 6.57 (d, J = 16.3 Hz, 2.5H, ethene), 6.07 (s, 2.5H, -CH=C(R)CH(CHO)-), 5.72 (d, J = 8.2 Hz, 2.5H, =CH-CH(O)-), 5.55 (d, J = 8.0 Hz, 1H, =CH = C(O)-), 2.68 (br, 5H, CH_2), 2.37 (s, 3H, CH_3), 2.36 (s, 7.5H, CH_3), 2.28 (s, 5H, CH_2), 2.26 (s, 2H, CH_2), 2.24 (br, 2H, CH_2), 1.00 (s, 15H, CH_3), 0.96 (s, 6 H, CH_3). ^{13}C NMR (150 MHz, acetone-d_6): δ 190.1, 189.3, 157.2, 156.8, 148.1, 147.9, 136.2, 136.1, 131.8, 131.6, 129.1, 128.3, 128.1, 127.8, 127.0, 126.6, 126.1, 126.0, 125.7, 124.1, 124.0, 120.3, 120.1, 120.0, 119.6, 119.0, 118.9, 112.5, 109.7, 46.6, 39.5, 39.3, 39.2, 31.5, 31.4, 28.44, 28.37, 9.9. IR (λ_{max}, cm^{-1}, KBr): 3452 (CH), 2948 (CH), 1645 (C = O), 1566 (C = C). MALDI-TOF: 382 $[M+H]^+$.

2.2.3.2. (E,Z)-2-(5,5-Dimethyl-3-((E)-2-(1-methyl-2-phenylindolizin-3-yl) vinyl)cyclohex-2-en-1-ylidene)acetaldehyde (**7b**).

Yield: 0.30 g (81%). Dark red powder, mp 75-77^0 C. R_f = 0.42 (hexane:ethyl acetate = 10:3).

^{1}H NMR (500 MHz, acetone-d_6): δ 10.10 (d, J = 7.9 Hz, 1H, CHO), 10.03 (d, J = 8.1 Hz, 2.5H, CHO), 8.55 (d, J = 7.0 Hz, 1H, H-5 indolizine), 8.54 (d, J = 7.0 Hz, 2.5H, H-5 indolizine), 7.54-7.48 (m, 10.5H, *m*-Ph, H-8 indolizine), 7.45-7.43 (m, 3.5H, *p*-Ph), 7.42-7.38 (m, 7H, *o*-Ph), 7.15 (d, J = 16.3 Hz, 3.5H, ethene), 7.09 (s, 1H, -CH=C(R)CH(CHO)-), 7.15 (d, J = 16.3 Hz, 3H, ethene), 7.10 (s, 2.5H, -CH=C(R)CH(CHO)-), 6.86 (dd, J = 8.9, 6.5 Hz, 3.5H, H-7 indolizine), 6.74 (dd, J = 7.0, 6.5 Hz, 3.5H, H-6 indolizine), 6.64 (d, J = 16.3 Hz, 1H, ethene), 6.52 (d, J = 16.3 Hz, 2.5H, ethene), 6.04 (s, 2.5H, -CH=C(R)CH(CHO)-), 5.73 (d, J = 8.1 Hz, 2.5H, =CH-CH(O)-), 5.58 (d, J = 7.9 Hz, 1H, =CH = CH(O)-), 2.72 (s, 2.5H, CH_2), 2.71 (s, 2.5H, CH_2), 2.35 (s, 5H, CH_2), 2.33 (s, 2H, CH_2), 2.28 (s, 1H, CH_2), 2.27 (s, 1H, CH_2), 2.21 (s, 3H, CH_3), 2.20 (s, 7.5H, CH_3), 1.02 (s, 15H, CH_3), 0.98 (s, 6 H, CH_3). ^{13}C NMR (100 MHz, acetone-d_6): δ 190.3, 189.2, 156.8, 156.3, 147.5, 147.4, 136.5, 136.4, 133.7, 132.0, 131.3, 131.2, 129.18, 129.16, 128.2, 127.9, 126.8, 126.7, 125.5, 124.6, 124.5, 121.1, 119.9, 119.8, 119.6, 118.71, 118.67, 118.3, 112.6, 110.6, 110.4, 46.5, 39.4, 39.10, 39.06, 31.5, 31.4, 28.4, 28.3, 9.1, 9.0. IR (λ_{max}, cm^{-1}, KBr): 3457 (CH), 2924 (CH), 1651 (C = O), 1561 (C = C). MALDI-TOF: 382 $[M+H]^+$.

2.2.4. (E,E,E,E)/(E,E,Z,E) 2-(3-Cyano-4-(-3-(5,5-dimethyl-3-(2-(3(1)-methyl-2-phenylindolizin-1(3)-yl)vinyl)cyclohex-2-en-1-ylidene)prop-1-en-1-yl)-5,5-dimethylfuran-2(5 H)-ylidene)malononitriles (**(MPI-1)-OT-TCF, (MPI-3)-OT-TCF)**

To solution of aldehyde 7 (0.20 g, 0.52 mmol) in dry ethanol (5 mL) solution of Me-TCF (0.10 g, 0.50 mmol) in dry ethanol (1 mL) was added, and combined solution was refluxed for 8 h. After removing the solvent the residue was purified by column chromatography (eluent: methylene chloride).

2.2.4.1. (E,E,E,E)/(E,E,Z,E) 2-(3-Cyano-4-(3-(5,5-dimethyl-3-(2-(3-methyl-2-phenylindolizin-1-yl)vinyl)cyclohex-2-en-1-ylidene)prop-1-en-1-yl)-5,5-dimethylfuran-2(5 H)-ylidene)malononitrile (**(MPI-1)-OT-TCF**).

Yield: 0.16 g (56%). Black powder. R_f = 0.3 (hexane:ethyl acetate = 2:1). ^{1}H NMR (600 MHz, DMSO-d_6): δ 8.22 (d, J = 6.8 Hz, 1H, H-5 indolizine), 8.09 (d, J = 8.9 Hz, 1H, H-8 indolizine), 7.96 (dd, J ~ 14, 13 Hz, 1H, =CH-CH = CH-TCF), 7.54 (dd, J = 7.6, 7.4 Hz, 2H, *m*-Ph), 7.46 (dd, J = 7.4, 7.4 Hz, 1H, *p*-Ph), 7.36 (d, J = 7.6 Hz, 2H, *o*-Ph), 7.29 (d, J = 15.9 Hz, 1H, ethene), 7.16 (dd, J = 8.9, 6.7 Hz, 1H, H-7 indolizine), 6.96 (dd, J = 6.8, 6.7 Hz, 1H, H-6 indolizine), 6.53 (d, J = 15.9 Hz, 1H, ethene), 6.41 (d, J ~ 13 Hz, 1H, ethene), 6.39 (d, J ~ 14 Hz, 1H, ethene), 6.27 (br, 1H, -CH=C(R)CH(CH = CHTCF)-), 2.41 (s, 2H, CH_2), 2.34 (s, 5H, CH_2, CH_3), 1.66 (s, 6H, CH_3), 0.95 (s, 6H, CH_3). ^{13}C NMR (150 MHz, DMSO-d_6): δ 177.0, 172.8, 156.1, 151.5, 143.7, 134.4, 132.6, 130.4, 128.4, 128.1, 127.3, 127.1, 124.9, 124.6, 121.5, 121.6, 118.2, 114.1, 113.7, 113.1, 112.9, 112.8, 109.9, 97.3, 90.1, 49.9, 38.3, 31.0, 27.9, 25.7, 9.6. ^{1}H NMR (400 MHz, $CDCl_3$): δ 8.20 (dd, J ~ 14, 14 Hz, 1H, =CH-CH = CH-TCF), 7.99 (dd, J ~ 14, 14 Hz, 3.3 H, =CH-CH = CH-TCF), 7.84-7.79 (m, 8.6H, H-5,8-indolizine), 7.53-7.48 (m, 8.6H, *m*-Ph), 7.46-7.40 (m, 4.3H, *p*-Ph), 7.38-7.34 (m, 8.6 H, *o*-Ph), 7.17 (d, J ~ 16 Hz, 1H, ethene), 7.16 (d, J = 15.9 Hz, 3.3H, ethene), 7.04-6.98 (m, 4.3 H, H-7 indolizine), 6.81-6.77 (m, 4.3H, H-6 indolizine), 6.56 (s, 1H, -CH=C(R)CH(CH = CHTCF)-), 6.53 (d, J = 16.1 Hz, 4.3 H, ethene), 6.26 (d, J = 12.5 Hz, 3.3H, ethene), 6.15 (d, J = 14.4 Hz, 4.3 H, ethene), 6.11 (s, 1H, -CH=C(R)CH(CH = CHTCF)-), 6.01 (d, J ~ 12 Hz, 1H, ethene), 2.39 (s, 6.6H, CH_2), 2.38 (br, 12.9 H, CH_3), 2.32 (s, 6.6H, CH_2), 2.29 (br, 4H, CH_2), 1.68 (s, 6H, CH_3), 1.65 (s, 19.8 H, CH_3), 1.02 (s, 19.8H, CH_3), 0.99 (s, 6H, CH_3). ^{13}C NMR (100 MHz, $CDCl_3$): δ 176.5, 173.0, 172.6, 156.3, 155.7, 151.0, 150.2, 144.1, 143.2, 135.0, 134.9, 132.4, 132.3, 130.8, 128.5, 128.4, 128.1, 127.6, 127.5, 127.4, 127.1, 125.8, 125.6, 124.5, 123.1, 123.0, 120.8, 120.5, 120.3, 120.2, 118.3, 118.2, 114.1, 113.5, 113.1, 113.0, 112.6, 112.4, 112.3, 112.2, 110.1, 109.9, 96.5, 96.3, 92.6, 92.1, 53.9, 53.4, 47.1, 39.9, 39.5, 39.1, 31.7, 31.4, 28.5, 28.2, 26.6, 9.9. IR (λ_{max}, cm^{-1}, KBr): 3506 (CH), 2219 (C≡N), 1562 (C = C). MALDI-TOF: 563 $[M+H]^+$.

2.2.4.2. (E,E,E,E)/(E,E,Z,E) 2-(3-Cyano-4-(3-(5,5-dimethyl-3-(2-(1-methyl-2-phenylindolizin-3-yl)vinyl)cyclohex-2-en-1-ylidene)prop-1-en-1-yl)-5,5-dimethylfuran-2(5 H)-ylidene)malononitrile (**(MPI-3)-OT-TCF**).

Yield: 0.20 g (71%). Black powder. R_f = 0.42 (hexane:ethyl acetate = 2:1). ^{1}H NMR (400 MHz, DMSO-d_6): δ 8.81 (d, J = 7.1 Hz, 1H, H-5 indolizine), 7.92 (dd, J ~ 14, 14 Hz, 1H, =CH-CH = CH-TCF), 7.60 (d, J = 8.9 Hz, 1H, H-8 indolizine), 7.54 (dd, J = 7.8, 7.5 Hz, 2H, *m*-Ph), 7.50-7.44 (m, 1H, *p*-Ph), 7.38-7.35 (m, 2H, *o*-Ph), 7.34 (d, J ~ 16 Hz, 1H, ethene), 7.06 (dd, J = 8.9, 6.8 Hz, 1H, H-7 indolizine), 6.89 (dd, J ~ 7.1,

6.8 Hz, 1H, H-6 indolizine), 6.42-6.35 (m, 3H, ethene), 6.11 (br, 1H, -CH=C(R)CH(CH = CH-TCF)-), 2.40 (s, 2H, CH_2), 2.39 (s, 2H, CH_2), 2.14 (s, 3H, CH_3), 1.66 (s, 6H, CH_3), 0.96 (s, 6H, CH_3). ^{13}C NMR (100 MHz, DMSO-d_6): δ 176.9, 172.5, 155.2, 150.7, 143.3, 134.8, 134.6, 132.3, 130.0, 128.6, 127.6, 127.5, 125.1, 124.7, 121.1, 121.0, 120.5, 117.7, 114.5, 113.7, 113.0, 112.9, 112.7, 112.2, 97.3, 90.4, 50.1, 38.2, 30.9, 27.9, 25.7, 8.7. ^{1}H NMR (600 MHz, $CDCl_3$): δ 8.35 (d, $J\sim7$ Hz, 1H, H-5 indolizine), 8.29 (d, J = 6.9 Hz, 3.5H, H-5 indolizine), 8.23 (dd, $J\sim15$, 12 Hz, 1H, =CH-CH = CH-TCF), 7.98 (dd, $J\sim14$, 13 Hz, 3.5H, =CH-CH = CH-TCF), 7.50 (dd, J = 7.8, 7.5 Hz, 9H, *m*-Ph), 7.45-7.41 (m, 9H, *p*-Ph, H-8 indolizine), 7.35 (d, J = 7.8 Hz, 9H, *o*-Ph), 7.14 (d, $J\sim16$ Hz, 1H, ethene), 7.06 (d, J = 16.1 Hz, 3.5H, ethene), 6.93-6.88 (m, 4.5H, H-7 indolizine), 6.80-6.76 (m, 1H, H-7 indolizine), 6.74 (dd, $J\sim6.9$, 6.7 Hz, 3.5H, H-6 indolizine), 6.60 (br, 1H, -CH=C(R)CH (CH = CHTCF)-), 6.46 (d, J = 16.1 Hz, 3.5H, ethene), 6.43 (d, $J\sim16$ Hz, 1H, ethene), 6.25 (d, J = 12.5 Hz, 3.5H, ethene), 6.16 (d, J = 14.5 Hz, 3.5H, ethene), 6.11 (d, $J\sim15$ Hz, 1H, ethene), 6.08 (s, 3.5H, -CH=C(R)CH(CH = CHTCF)-), 6.02 (d, $J\sim12$ Hz, 1H, ethene), 2.39 (s, 7H, CH_2), 2.30 (s, 7H, CH_2), 2.29 (s, 2H, CH_2), 2.25 (s, 2H, CH_2), 2.22 (s, 13.5H, CH_3), 1.67 (s, 6H, CH_3), 1.65 (s, 21H, CH_3), 1.02 (s, 21H, CH_3), 0.98 (s, 6H, CH_3). ^{13}C NMR (150 MHz, $CDCl_3$): δ 176.4, 176.3, 172.8, 172.6, 155.4, 155.1, 149.8, 149.5, 143.8, 143.0, 135.2, 134.9, 134.8, 133.2, 133.1, 130.5, 129.3, 128.5, 127.6, 127.5, 125.0, 124.8, 124.5, 124.0, 123.8, 121.0, 120.8, 120.5, 120.3, 120.3, 119.7, 119.5, 118.0, 117.8, 114.5, 113.6, 113.0, 112.8, 112.6, 112.4, 112.3, 112.1, 112.0, 111.9, 96.5, 96.4, 92.6, 54.2, 46.9, 39.8, 39.0, 31.6, 31.4, 28.4, 28.2, 26.5, 9.0. IR (λ_{max}, cm^{-1}, KBr): 2925 (CH), 2221 (C≡N), 1561 (C = C). MALDI-TOF: 563 $[M+H]^+$.

2.3. Computational details

All density functional theory (DFT) calculations were performed with the Gaussian 16 program package [41]. In general the spherical def2-TZVP atomic orbital (AO) basis set was used [42,43]. All the structures were optimized with the use of long-range corrected CAM-B3LYP [44] functional. The nature of $S_0 \rightarrow S_1$ transitions has been characterized by the analysis of the frontier molecular orbitals. Stationary points were characterized as minima by frequency analysis. Solvent effects on the photophysical properties have been taken into accounts using the polarizable continuum model (PCM) [45–49] within linear-response (LR) implemented in Gaussian 16 software. Time-dependent density functional response theory (TD-DFT) [45–52] has been employed to compute the vertical excitation energies (absorption wavelengths) and oscillator strengths on the ground state (GS) S_0 equilibrium geometries, each optimized in the gas phase as well as with the use of PCM model with standard parameters for dimethylsulfoxide (DMSO) as a solvent. All the excitations energies have been red-shifted by an error factor computed as the difference between $E_{S0\rightarrow S1}$ and corresponding experimental λ_{max} (0.6 eV) in order to better match the experimental spectral curves. Simulated electronic absorption spectra, calculated as 20 vertical excitations at the optimized ground state (GS) geometries were empirically broadened by single Gaussian type functions with full-width at half maximum (FWHM) equal to 0.4 eV. The dipole length representation is used to calculate oscillator strengths discussed in the present paper.

2.4. Fabrication and preparation of samples for determining the electro-optic characteristics

To determine the EO characteristics of composite materials, films with a thickness of 1.5–2 μm were fabricated. Films were spin-cast on glass substrates coated with an ITO layer from 20% PMMA solutions in cyclohexanone, containing the calculated amount (10 and 15 wt%) of the chromophore, at a centrifuge rotation speed of 5000 rpm for 45 s. To remove residual solvent two modes of samples drying were used. First: the samples were kept in a vacuum oven at room temperature for 10–16 hours. Second: the samples were first kept in a vacuum oven at room temperature for 10–16 h, and then at 60 °C for 2.5 h. To achieve noncentrosymmetric structure of the material, poling was performed, during which the chromophores were oriented along the direction of the applied dc electric field. In the case of the studied polymer films, poling was carried out in the corona discharge field at the hand-made corona triode; the so-called “positive corona” was used. The voltage on the corona electrode (tungsten needle) was equal to 8 kV, the distance from the grid to the cathode was 10 mm, the voltage on the grid was 1.2 kV. The corona field was applied to samples heated to a temperature T_p, which is slightly higher than the glass transition temperature T_g of the polymer. In this state the sample was kept for 20 min, then cooled to room temperature during one hour, after that the field was turned off. The quality of orientation was controlled by the absorption change in UV–vis spectra detected before and after poling, and characterized by order parameter, η, calculated by the following formula:

$$\eta = 1 - A/A_0$$

where A and A_0 are the absorptions of the polymer films after and before poling. After poling, a second silver or aluminum electrode with a diameter of (D) 6 mm and a thickness of ~ 50 nm was deposited on the surface of the polymer by thermal spraying. The role of the first electrode is played by the ITO layer.

3. Results and discussion

3.1. Synthesis, NMR study and thermal properties

The synthetic procedures for the title chromophores are shown in Scheme 1. Isomeric 3(1)-methyl-2-phenylindolizine-1(3)-carbaldehydes (**4a,b**) [31,53,54] have been synthesized in four steps starting from acetophenone (**1a**) and propiophenone (**1b**). Further three steps consisting of condensation of aldehydes **4** with isophorone, reaction of ketones **5** with diethyl cyanomethylphosphonate and reduction of nitriles **6** by diisobutylaluminium hydride lead to π-extended aldehydes **7**. Final Knoevenagel condensation of aldehydes **7a** and **7b** with **Me-TCF** [55] results in chromophores (**(MPI-1)-OT-TCF** and **(MPI-3)-OT-TCF**, respectively. Ketons **5** are *trans*-isomers, while the compounds **6a,b** are cis/trans-isomer mixture, E/Z (Z/E) = 1 : ~1.5. The ratio of the Z : E isomers for the compounds **7a,b** calculated by ^{1}H NMR spectra is 1 : 2.5. A similar trend has been observed in ^{1}H NMR spectra in chromophores with aniline [56] or julolidine [8] donors with the same π-bridge and acceptor. Chromophores (**(MPI-1)-OT-TCF** and **(MPI-3)-OT-TCF**) exist in two forms in $CDCl_3$ solution, according to NMR data. However, there are no doubling of proton and carbon signals in the ^{1}H and ^{13}C NMR spectra of chromophores (**(MPI-1)-OT-TCF** and **(MPI-3)-OT-TCF**) in DMSO-d_6 as well as in DMF-d_7.

More detailed ^{1}H NMR study was performed for the chromophore **(MPI-3)-OT-TCF**. In all polar solvents such as DMSO-d_6, DMF-d_7, and CD_3CN one chromophore isomer has been observed. Two isomers exist in solvents with low polarity, in dioxane-d_{10} and $CDCl_3$ giving almost doubling of all signals except the signals of the phenyl group and other 1–2 signals. Solvent polarity increase up to moderately polar CD_2Cl_2 results in the doubling of only two signals: these are proton signals at 6 and 7 carbon atoms of π-bridge (Scheme 1) which appear as broadened ones. As for the ratio of isomers, it varies slightly and is equal to 2.7:1, 3.5:1 and 4:1 in dioxane, chlorophorm and dichlorometane, correspondingly (Fig. 1). Thus for solutions of chromophores (**(MPI-1)-OT-TCF** and **(MPI-3)-OT-TCF**), two isomers degenerate with the polarity increase, turning into one isomer. This behavior of chromophores (**(MPI-1)-OT-TCF** and **(MPI-3)-OT-TCF**) is quite different from that of their precursors **6a,b** and **7a,b**, for which the ratio of two isomers is constant and does not change with solvent. It should be noted that after removing chloroform-*d* and re-recording the ^{1}H NMR spectrum in dimethylformamide-d_7, the spectrum corresponds to a single isomer. Conversely, removal of dimethylformamide and re-recording the ^{1}H

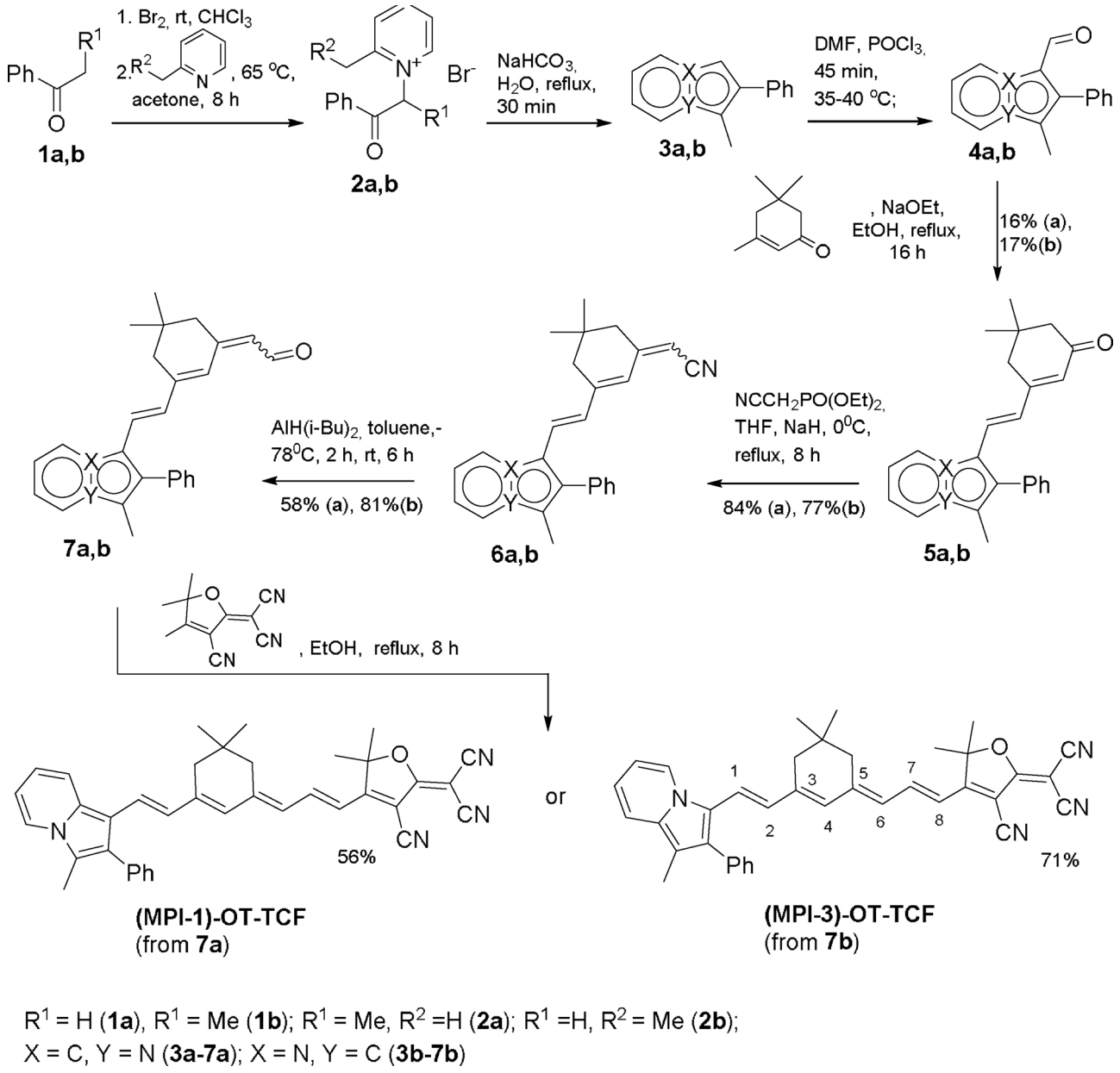

Scheme 1. Synthesis of two isomers ((**MPI-1)-OT-TCF** and **(MPI-3)-OT-TCF**) of indolizine-based chromophores with octatetraene π-bridge and tricyanofurane acceptor.

NMR spectrum again in chloroform leads to both isomers occurrence with the same (3.5:1) ratio.

The indolizine-based chromophores have high thermal stability: the decomposition temperatures at which 5% mass loss occurs at heating are above 270 °C (values T_d^a in Table 1, Fig. 2). This agrees well with temperatures of thermal decomposition, detected by DSC (values T_d^b in Table 1, Fig. 3) and data of the first derivative (values T_d^c in Table 1). The chromophores appeared as highly crystalline compounds with a melting point at 255 °C and 262 °C for **(MPI-1)-OT-TCF** and **(MPI-3)-OT-TCF**, respectively (Fig. 3).

3.2. Photophysical properties

None of the synthesized compounds demonstrates detectable emission in solutions. The electronic absorption spectra of solutions of the synthesized compounds in organic solvents of different polarity are presented in Fig. 4.

In the spectra of both systems in the least polar dioxane solutions broad, symmetric and highly intensive (extinction coefficients ε ~ 3–6·10^4 L·Mol^{-1}·cm^{-1}) the lowest-energy absorption bands with maxima (λ_{max}) at ~690-800 nm dominate, with the edges spreading up to 1000 nm (Fig. 4, Table 2). A replacement of MPI-1 fragment of **(MPI-1)-OT-TCF** by MPI-3 results in the red-shift of λ_{max} of **(MPI-3)-OT-TCF** by 0.05 eV, similar to the case of previously described closely related systems [31,57,58]. The spectra registered in moderately polar dichloromethane and chloroform solutions demonstrate a rather large positive solvatochromic shift and the strongest absorption band broadening relative to that in dioxane solutions. These effects are accompanied by appearing of shoulders at ca. 880–950 nm. For solutions in more polar acetonitrile an opposite, negative solvatochromic shift takes place, and the shoulder at longer wavelengths becomes more evident. In the spectra of the most polar DMF and DMSO solutions, the shoulder transforms into a separate narrow band (λ_{cyan}), best resolved from the main peak in the case of DMSO solution. It should be noted that, in contrast to acetonitrile solution, maximum of the strongest band (λ_{max}) in the spectra of both compounds in DMF and DMSO undergoes

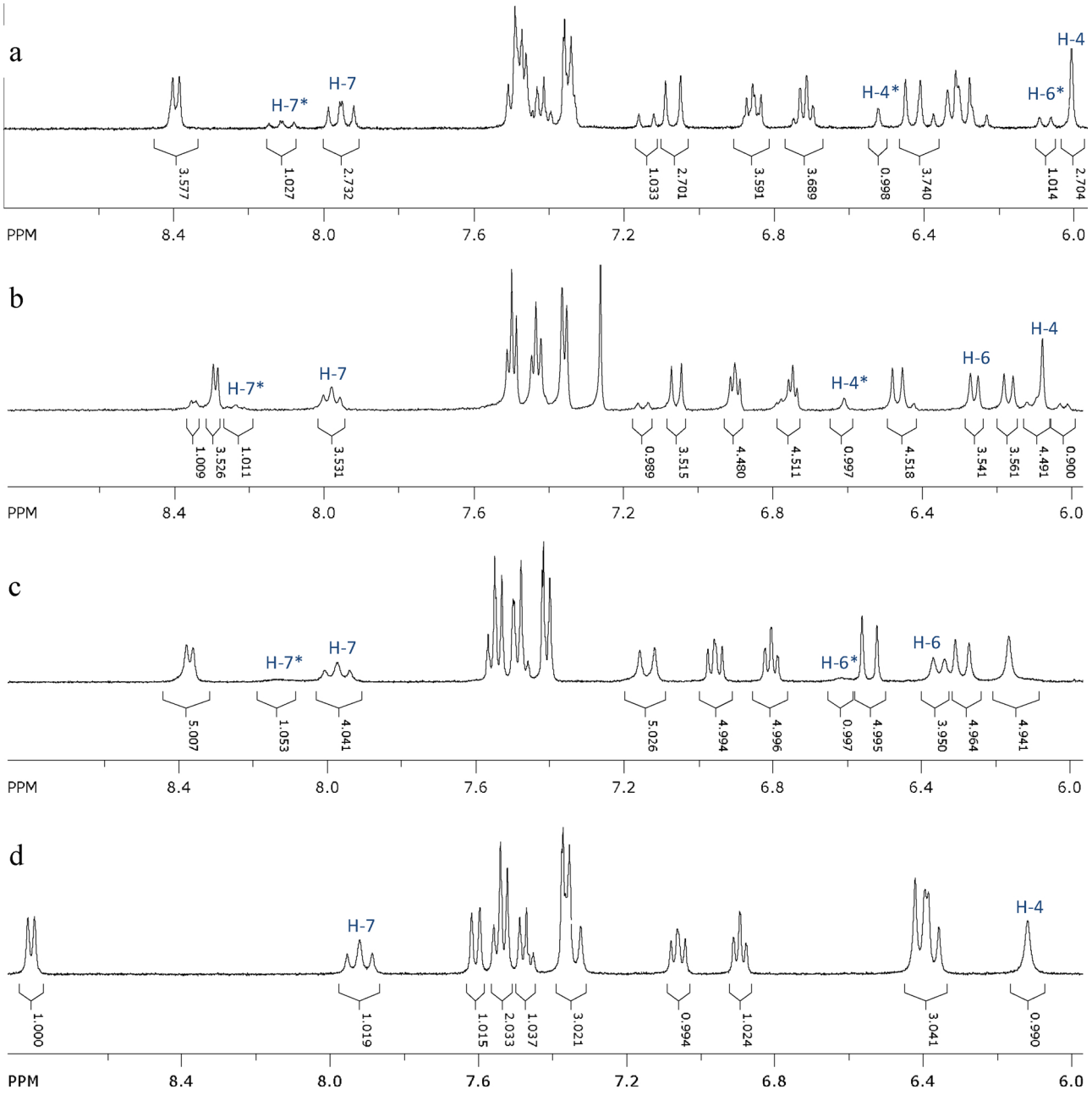

Fig. 1. ^{1}H NMR (6.0–8.8 ppm) spectra of **(MPI-3)-OT-TCF**) in dioxane-d_{10} (a), chloroform-d (b), dichloromethane-d_2 (c), dimethylsulfoxide-dd_6(d). The numbering of protons is made according to Scheme 1.

Table 1
Thermal properties of the studied chromophores.

Chromophore	(MPI-1)-OT-TCF	(MPI-3)-OT-TCF
T_d^a, °C	270	273
T_d^b, °C	262	268
T_d^c, °C	288	280
T_m^d, °C	255	262

T_d - decomposition temperature: [a] TGA, temperature at which 5% mass loss occurs at heating, [b] DSC, [c] dTGA, [d]T_m – melting point (from DSC data).

positive solvatochromic shift (Table 2).

Such inversion of solvatochromism from positive upon transition from dioxane to chloroform (methylene chloride) to negative upon transition from chloroform (methylene chloride) to acetonitrile (DMF) is rather typical for many D-π-A chromophors. The value of positive solvatochromism for chromophores with a TCF acceptor fragment and with the octatetraene π-bridge is noticeably greater than the value of the negative solvatochromic effect [59,60]. The same pattern is found for **(MPI-1)-OT-TCF** and **(MPI-3)-OT-TCF**: positive solvatochromism upon transition from dioxane to chloroform (88–91 nm or 0.19 eV) significantly prevails over negative (37–38 nm or 0.09-0.12 eV) upon transition from chloroform) to acetonitrile. A stronger negative solvatochromic effect (but not superior to positive) is demonstrated by chromophores with a thiophene [61,62] or quinoxaline-2-one cores in π-bridge [63]. Chromophores with an aromatic quinoxaline moiety are even characterized by the predominance of a negative solvatochromic effect over a positive [64].

According to the published works, the λ_{cyan} band could be ascribed to the so-called “cyanine limit” structure (CLS) with a vanishing bond-length alternation (BLA) upon a certain ratio between the electron-donating and withdrawing motifs. CLS is characterized by sharp,

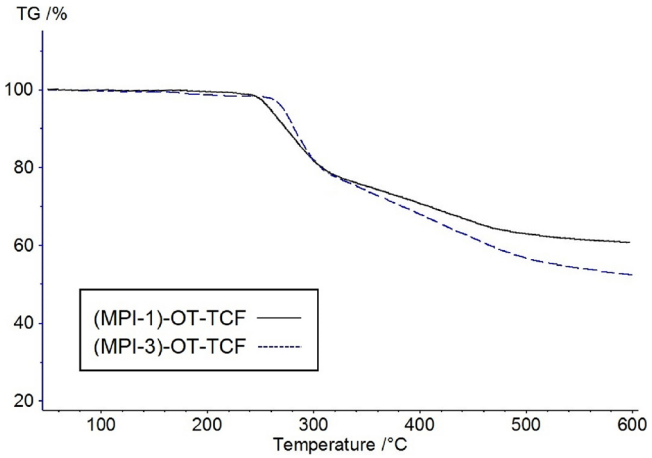

Fig. 2. TGA curves for **(MPI-1)-OT-TCF** and **(MPI-3)-OT-TCF**.

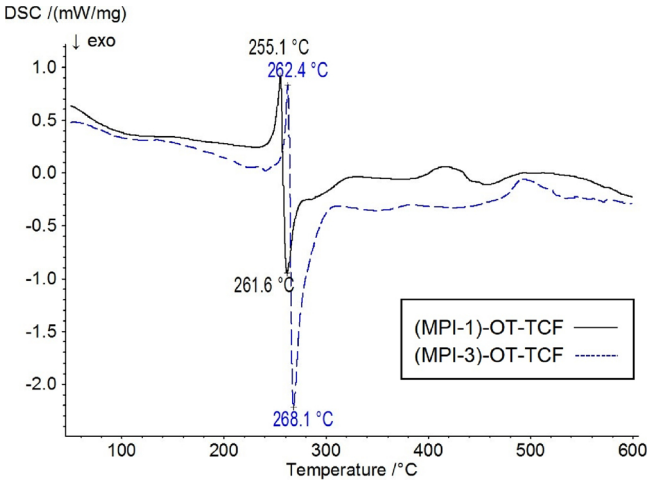

Fig. 3. DSC curves for **(MPI-1)-OT-TCF** and **(MPI-3)-OT-TCF**.

intense absorption band shifted toward red-NIR spectral region [65]. In particular, it was shown that increasing the solvent polarity for the push-pull molecules with large values of ground-state dipole moments may lead to the cross of cyanine limit [66]. Other strategies to reach the cyanine limit are based on the chemical modifications of donor/acceptor strength or lengthening of conjugated skeleton. In the intermediate case the coexistence of two forms ascribed to symmetrical and asymmetrical distributions of charge density takes place [66].

It should be noted that indolizine-based compounds **(MPI-1)-OT-TCF** and **(MPI-3)-OT-TCF** demonstrate a presence of CLS in acetonitrile and probably even in dichloromethane and chloroform solutions, while related systems with julolidine donor fragment [7,9] do not reveal any sign of CLS under the same conditions. This feature, as well as red shift of electronic absorption bands of the considered systems compared to their aniline analogs [56,67], indicates better donating properties of indolizine unit as mentioned earlier [28].

To better understand the origin of electronic absorption spectra of **(MPI-1)-OT-TCF** and **(MPI-3)-OT-TCF**, quantum chemical calculations within DFT and time-dependent DFT (TD-DFT) approach have been performed. According to our experience, [68–70], both hybrid PBE0 [71,72] and long-range corrected CAM-B3LYP [73] functionals are suitable for electronic spectra simulation of D-π-A systems related to present compounds. CAM-B3LYP simulations, in spite of systematic overestimation of vertical excitations energies, typically reproduce relative intensities of absorption bands in spectra of such systems [74] better. For this reason CAM-B3LYP functional was used for simulation of spectra of isolated molecules **(MPI-1)-OT-TCF** and **(MPI-3)-OT-TCF**, which are compared to the experimental spectra of the least polar dioxane solutions of the compounds in Fig. 5.

The simulated spectra match their experimental counterparts quite well, demonstrating that the strongest absorption band should be associated with the only $S_0 \rightarrow S_1$ electronic transition. This transition from the highest occupied (HOMO) to the lowest unoccupied (LUMO) molecular orbitals has the largest value of oscillator strength ($f \sim 2.0–2.5$) over all the calculated transitions shown in Fig. 5. Intramolecular charge-transfer character of the HOMO-LUMO transition is seen from Fig. 6: electronic density migrates from electron-donor indolizine moiety to TCF acceptor simultaneously involving π-bridging motifs.

Effect of high polarity of solvent on characteristics of **(MPI-1)-OT-TCF** and **(MPI-3)-OT-TCF** has been simulated with the use of polarizable continuum model (PCM) [75–77] with standard parameters implemented in Gaussian 16 for DMSO. HOMOs and LUMOs obtained using this implicit solvation model (Fig. S1 in ESI) practically coincide with the corresponding gas-phase orbitals shown in Fig. 6, the former HOMOs being only slightly more delocalized over the molecular backbone than the latter. Lengths of single and double CC bonds forming π-bridge, dipole moments (μ) and parameters of the lowest-energy electronic transition ($S_0 \rightarrow S_1$) calculated for the molecules, both isolated in vacuum and embedded in DMSO treated implicitly via PCM

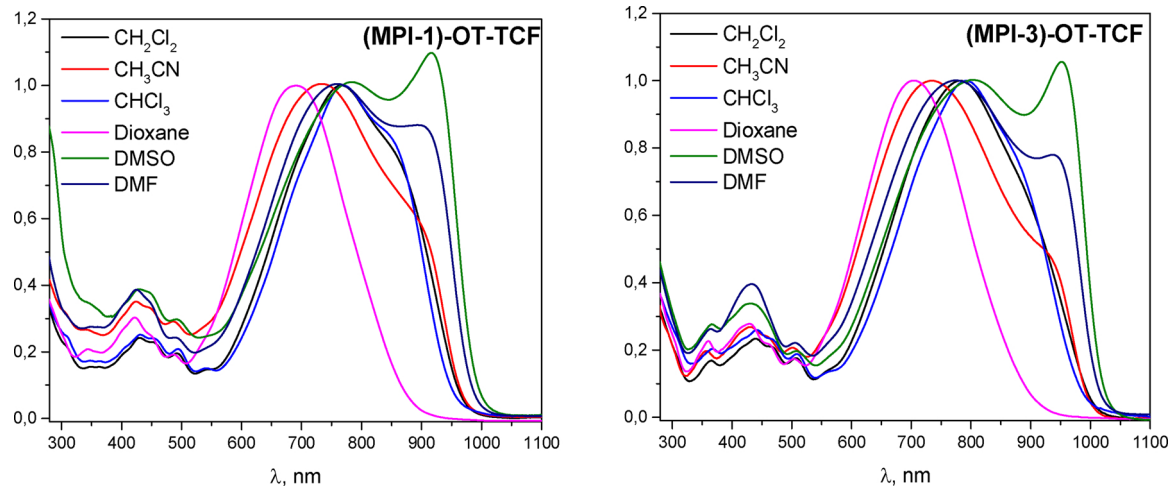

Fig. 4. Electronic absorption spectra of solutions of the considered systems (**(MPI-1)-OT-TCF**, **(MPI-3)-OT-TCF** in 1,4-dioxane (Dioxane), dichloromethane (CH_2Cl_2), chloroform ($CHCl_3$), acetonitrile (CH_3CN), *N,N*-dimethylformamide (DMF) and dimethylsulfoxide (DMSO). Presented relative absorption intensities were normalized to unity for the most intensive and broadest bands.

Table 2
Experimental photophysical data on the maxima positions of the strongest and broadest electronic absorption band (λ_{max}) and additional absorption band in the near-IR region (λ_{cyan}) appearing in polar solvents, the corresponding transitions energies (E), and extinction coefficients (ε) measured for solutions of **(MPI-1)-OT-TCF** and **(MPI-3)-OT-TCF** in 1,4-dioxane, dichloromethane, chloroform, acetonitrile, DMF and DMSO.

chromophore		Solvent					
		Dioxane	CH_2Cl_2	$CHCl_3$	CH_3CN	DMF	DMSO
(MPI-1)-OT-TCF	λ_{max},[a] nm	688	765	769	731	760	785
	E, eV	1.80	1.62	1.61	1.70	1.63	1.58
	ε, $L{\cdot}Mol^{-1}{\cdot}cm^{-1}$	43000	51000	51000	35000	31500	40000
	λ_{cyan},[b] nm	–	883	875	913	914	915
	E, eV	–	1.40	1.42	1.36	1.36	1.36
(MPI-3)-OT-TCF	λ_{max},[a] nm	704	782	792	735	777	801
	E, eV	1.76	1.59	1.57	1.69	1.60	1.55
	ε, $L{\cdot}Mol^{-1}{\cdot}cm$-	51500	51500	56500	40000	39000	42000
	λ_{cyan},[b] nm	–	915	900	944	948	951
	E, eV	–	1.36	1.38	1.31	1.31	1.30

[a] – λ_{max} is ascribed to the lowest-energy electronic absorption band.
[b] – λ_{cyan} corresponds to the position of shoulder at λ_{max} absorption band appearing in solutions $CH_3CNCH_2Cl_2$, $CHCl_3$, or of a sharp separate band appearing in DMF and DMSO and ascribed to the presence of the cyanine limit structure.

approximation, are summarized in Table 3. As seen from the table, C—C and C=C bonds tend to be equalized in DMSO, which is reflected in ca. 50% reduced BLA values. Furthermore, the calculated ground-state dipole moments (μ in Table 3) strongly increase with solvent polarity. This may lead to the cross of cyanine limit in polar solvents, what was observed experimentally. Our calculations do not demonstrate absolute equalization of single and double CC bonds in DMSO, but this effect is extremely difficult to be reproduced by quantum chemical computations [78]. Nevertheless, absorption wavelength computed for the structure optimized with the use of PCM model λ = 937/969 nm for both **(MPI-1)-OT-TCF/(MPI-3)-OT-TCF** matches reasonably well experimental λ_{cyan} = 915/951 nm.

Thus quantum-chemical calculations for isolated molecules show the presence of one form in non-polar dioxane solutions, while the analysis of the pronounced charge-transfer character of the first singlet excitations, the predicted large values of dipole moments notably increasing in highly polar media accompanied by bond length equalization, are in good agreement with the typical markers of CLS revealed in polar solvents for the systems under study. Simultaneous presence of sharp NIR absorptions, which should be assigned to the CLS, and broad strong bands similar to those registered in dioxane solutions strongly suggests a coexistence of two types of structures in polar media.

According to NMR data (vide supra), form **I** (with large BLA values) exists in low-polar dioxane and may be present even in chloroform solutions as a mixture of *E*- and ***Z***-isomers. The solvent polarity increase leads to the realization of the CLS form **II,** which may be accompanied by the zwitter-ionic form **III** (Fig. 7). The former should be characterized by low barriers for *E/Z* isomerization, while for the latter both *Z* and *E* structures represent simple conformers (rotamers). In any case, the signals of possible *Z* and *E* structures of **II** and **III** forms undergoing fast mutual transformations would be averaged in the NMR spectra recorded in acetonitrile, dimethylformamide and dimethylsulfoxide and would be indistinguishable from single isomeric structure. Thus, NMR spectroscopy data on isomeric composition of both compounds in polar media strongly suggest that two forms revealed by the UV–vis spectra analysis are **II** (CLS) and **III** (zwitter-ionic structure) ones.

3.3. Electrochemical study

The studied chromophores are characterized by irreversible oxidation and reduction waves. The estimations of the redox properties of the NLO chromophores studied by cyclic and differential pulse voltammetries (CV and DPV) are presented in Table 4 and Fig. 8. Oxidation proceeds very easily, practically at zero potentials (with refer to $Fc^{+/0}$).

To estimate the HOMO-LUMO energy gaps according to electrochemistry data we used recently proposed approach [79], where the oxidation and reduction potentials are shown to be closely related to the energies of the HOMO and LUMO levels of organic NLO chromophore. Due to irreversibility or low reversibility of redox processes we used potential values obtained by the DPV method (as the ones most close to the standard oxidation and reduction potentials) to calculate the frontier orbitals energy [79,80]:

$$E_{HOMO} = -(E[_{DPV,ox\ vs.\ Fc+/\ Fc}] + 4.8)(eV),$$

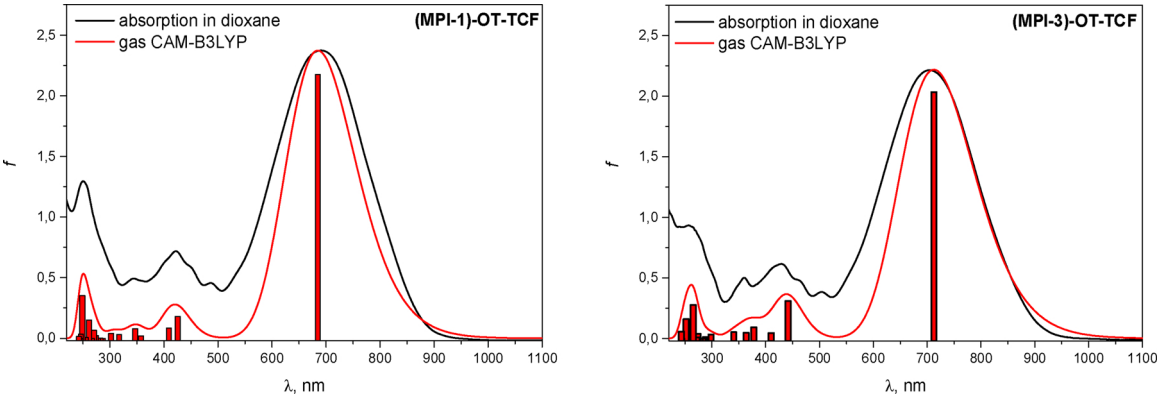

Fig. 5. Simulated (red) and experimental (black) absorption spectra of **(MPI-1)-OT-TCF** (left) and **(MPI-3)-OT-TCF** (right). Experimental spectra are registered for dioxane solutions. Simulated spectra are computed at CAM-B3LYP/def2-TZVP level. All the calculated electronic transitions are systematically red-shifted by 0.6 eV.

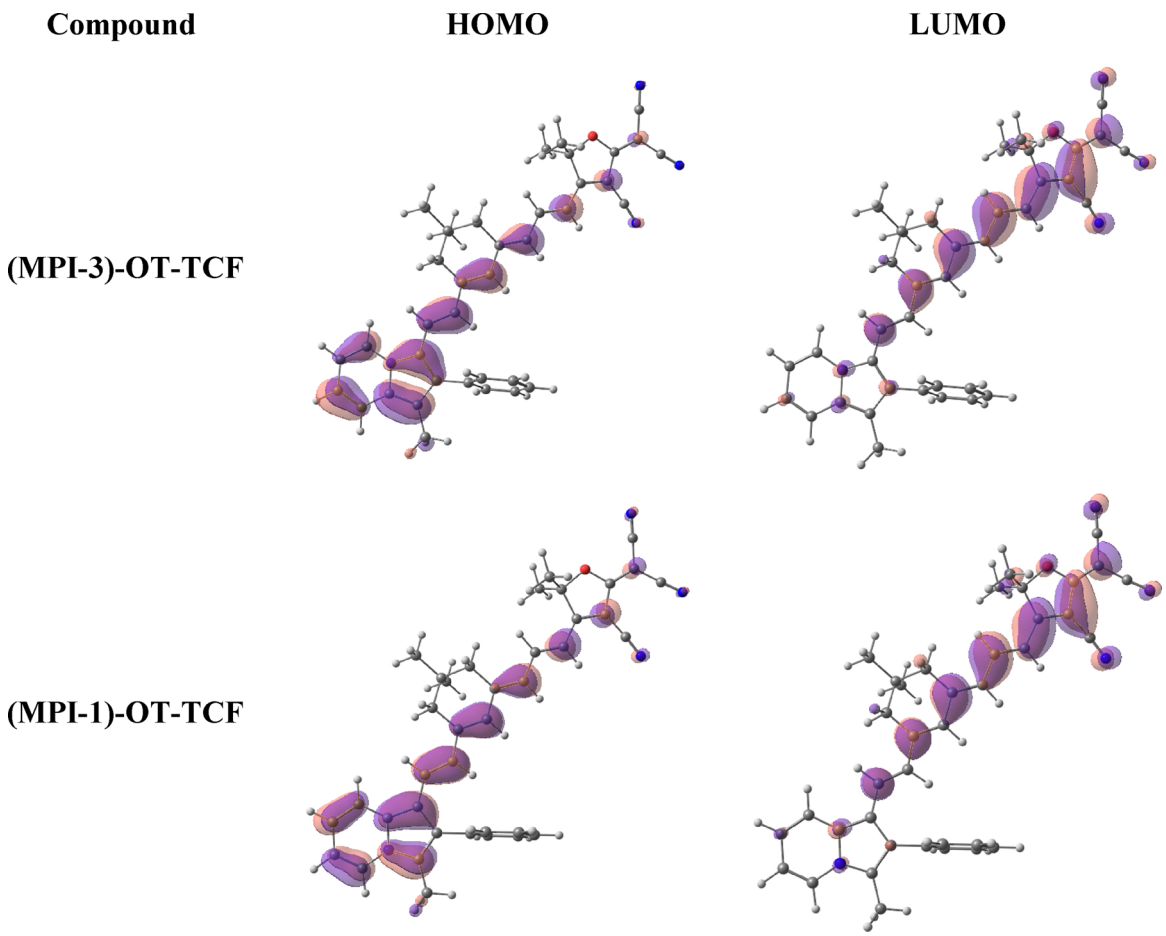

Fig. 6. HOMO and LUMO calculated for the optimized ground-state structures (gas phase).

$E_{LUMO} = -(E[_{DPV,red\ vs.\ Fc+/\ Fc}] + 4.8)(eV)$.

The following regularities were found: the studied chromophores have a low value of the difference in the energies between the frontier orbitals (about 0.8–0.9 eV), which is close to that for the best world analogues [1]; the energy gaps ΔE for compounds **(MPI-1)-OT-TCF** and **(MPI-3)-OT-TCF** are very close to each other in both solvents (CH_2Cl_2 and DMSO), what indicates that they have close polarizabilities; the dependence of the reduction potentials of the chromophores on the solvent is revealed, so, in DMSO, the reduction potentials are lower, and the change of solvent does not affect the oxidation potentials. This is reflected in ΔE values, that is, the difference in ΔE is determined by different reduction potentials in DMSO and CH_2Cl_2. So, the solvatochromic effect is confirmed by the experimental values of redox potentials. The estimation of the effect of the solvent (DMSO and CH_2Cl_2) on ΔE_{EC} (the energy gap) performed from electrochemical data is ca. 0.15 eV, what is close to solvatochromic effect ~ 0.21 eV determined on the basis of the absorption band shift.

3.4. EO performance

EO measurements were performed by ellipsometric Teng-Man technique [81]. EO coefficients, r_{33}, were calculated on the basis of measurements and set-up parameters according to the following formula [82].

$$r_{33} = \frac{3\lambda\sqrt{2}}{4\pi}\cdot\frac{1}{V_m}\cdot\frac{U_m}{\widetilde{U_C}}\cdot\frac{(n^2-\sin^2\theta)^{1/2}}{n^2\sin^2\theta} \quad (1)$$

where $\widetilde{U_c} = \frac{U_c^{max}}{2}$ – constant component of the output signal, λ – wavelength of the laser beam, V_m – modulating voltage applied to the film; n – refraction index; θ –angle of beam incidence on the sample. The value of r_{33} is obtained from the results of measurements of U_m and $\widetilde{U_c}$, the corresponding dependence has the form of an ellipse recorded with the fixed experimental parameters (λ, V_m, θ) and characteristics of the EO material (n); the length of its vertical axis (aperture) is proportional to the magnitude of the EO coefficient (Fig. 9); accuracy of determining the EO coefficient does not exceed 10%.

The samples were spin-cast on glass substrates covered with ITO, playing the role of the foot electrode, the upper electrode being either Ag or Al thermally sprayed on the film surface. Samples with 10 and 15 wt% chromophore content were prepared and poled in the corona-discharge field; the conditions of poling, mainly the poling temperature were chosen to be slightly higher than the materials T_g = 95 °C. The results of the EO coefficient measurements are presented in Table 5. The obtained results demonstrate the essential effect of the sample preparation on the r_{33} values. After spin-casting the films were dried in vacuum desiccator to remove residual solvent; two procedures were used: the films were dried either at room temperature for 10–16 h or at 60 °C switching on vacuum twice for 80 min.

The best results were obtained for the case when poling temperature was about 20 °C higher than T_g; the smaller was the T_p value, the lower was r_{33}. Surprisingly, the material **(MPI-3)-OT- TCF/PMMA** with chromophore content 10 wt% exhibited somewhat higher values of EO coefficient than those with 15 wt% of the chromophore, though one could expect the opposite situation keeping in mind the data for the guest-host CLD-1/PMMA material [56] with chromophore differing from **(MPI-3)-OT-TCF** by the donor group. Thus the presence of phenyl substituent in heterocyclic donor moiety of **(MPI-3)-OT-TCF** seems to result in the hindrance of reorientation during poling. The modification

Table 3
Selected structural and photophysical parameters of **(MPI-1)-OT-TCF** and **(MPI-3)-OT-TCF** calculated for isolated molecules in vacuum (gas) and in polarizable continuum (DMSO).

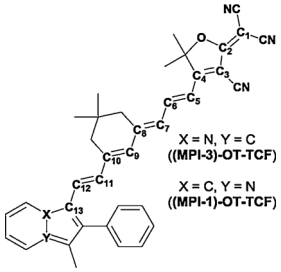

	(MPI-3)-OT-TCF			(MPI-1)-OT-TCF		
	gas Bond length Å	DMSO	Δgas-DMSO	gas Bond length Å	DMSO	Δgas-DMSO
C1 = C2	1.362	1.380	−0.018	1.362	1.381	−0.019
C2–C3	1.443	1.424	0.019	1.442	1.422	0.020
C3 = C4	1.363	1.384	−0.021	1.364	1.387	−0.023
C4–C5	1.422	1.398	0.024	1.421	1.396	0.025
C5 = C6	1.354	1.372	−0.018	1.355	1.375	−0.020
C6–C7	1.422	1.401	0.021	1.421	1.398	0.023
C7 = C8	1.358	1.376	−0.018	1.359	1.378	−0.019
C8–C9	1.434	1.418	0.016	1.433	1.416	0.017
C9 = C10	1.352	1.364	−0.012	1.353	1.366	−0.013
C10–C11	1.442	1.432	0.01	1.443	1.431	0.012
C11 = C12	1.346	1.354	−0.008	1.345	1.354	−0.009
C12–C13	1.432	1.420	0.012	1.437	1.425	0.012
BLA [a]	0.077	0.044	0.033	0.077	0.041	0.036
Characteristics of $S_0 \rightarrow S_1$ vertical excitation						
E [b] (eV)	2.34	1.88	0.46	2.41	1.92	0.49
λ [c] (nm)	530	659	−129	514	646	−132
f [d]	2.21	2.68	−0.47	2.37	2.77	−0.40
Dipole moments (μ), D						
	20.2	33.8	13.6	22.1	36.7	14.6

[a] The bond length alternation parameters (BLA) defined as a difference between the averaged bond lengths of single and double bonds presented in the table; [b] energy; [c] wavelength; [d] oscillator strength.

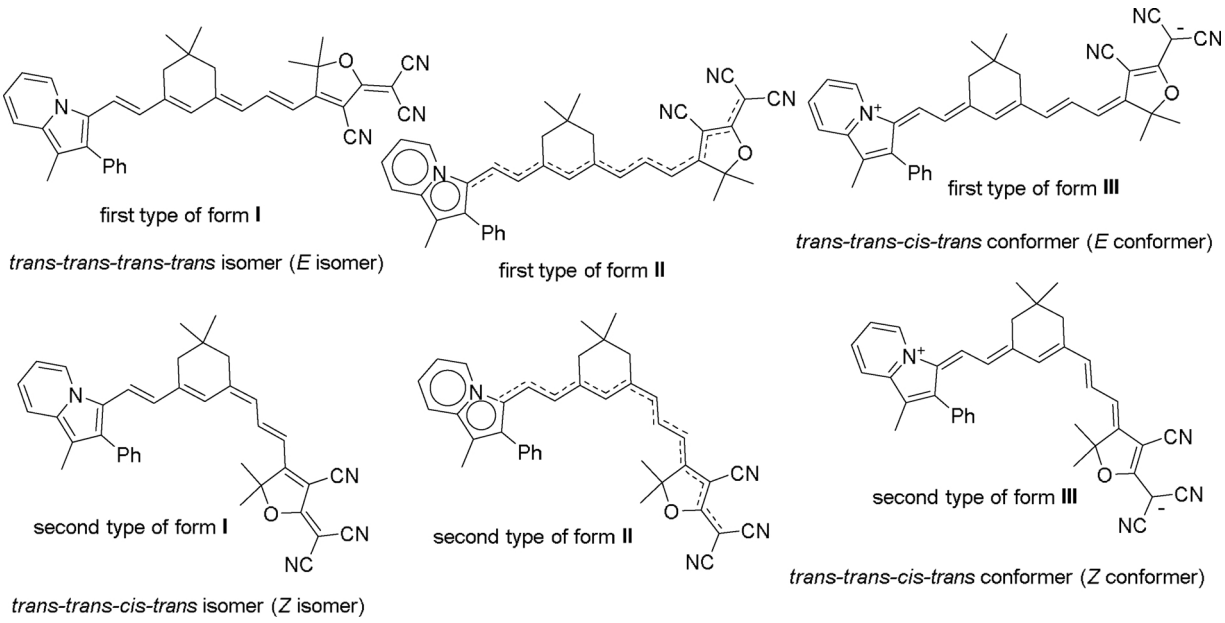

Fig. 7. Two isomer (conformer) forms and different resonance forms of chromophore **(MPI-3)-OT-TCF.**

of the indolizine donor group may eliminate the problem and permit increase of the chromophore content, what will result in higher EO coefficients. This assumption is supported by the fact that for CLD-1/PMMA material the optimal chromophore content is as high as 32 wt% and it results in rather high r_{33} value 85 pm/V [56], besides according to theoretical estimations performed at the M06-2X/aug-cc-pVDZ′ level **(MPI-3)-OT- TCF** demonstrated somewhat higher (by 5%) values of first hyperpolarizability than CLD-1 [30]. This assumption is in accordance with rather low values of order parameter (Fig. 10) for the case of the films with chromophore content 15 wt% in comparison with the case of 10 wt%.

These data motivate us to optimize poling conditions for **(MPI-3)-**

Table 4
Electrochemical data (CV peak potentials, DPV potentials) for oxidation-reduction of chromophores and calculated frontier orbitals energy values.

Chromophore	Cyclic votammetry (E, V)		DPV potentials (V)		E_{HOMO}, eV	E_{LUMO}, eV	ΔE_{EC}, eV
	Oxidation	Reduction	Oxidation	Reduction			
in CH_2Cl_2							
(MPI-3)-OT-TCF	E_p^f=-0.01; irrev.	E_p^f=-1.04; irrev.	−0.05	−0.96	−4.75	−3.84	0.91
(MPI-1)-OT- TCF	E_p^f = 0.02; irrev.	E_p^f=-1.07; irrev.	−0.02	−0.99	−4.78	−3.81	0.97
in DMSO							
(MPI-3)-OT- TCF	E_p^f=-0.01; irrev.	E_p^f=-0.91; irrev.	−0.06	−0.82	−4.74	−3.98	0.76
(MPI-1)-OT- TCF	E_p^f = 0.02; irrev.	E_p^f=-0.94; irrev.	−0.03	−0.85	−4.77	−3.95	0.82

Conditions: CH_2Cl_2/0.2 M Bu_4NBF_4 or DMSO/0.1 M Bu4NBF4, Pt working electrode; $AgNO_3$ reference electrode, substrate concentration 1–2 mM. Abbreviations: irrev.-irreversible; E_p^f - forward peak potential; $\Delta E_{EC} = E_{LUMO} - E_{HOMO}$.

OT-TCF/PMMA films, so as to improve the order parameter for the film with chromophore content of 15 wt% and to examine the effect of its further increase in future.

4. Conclusion

Chromophores with isomeric 1-methyl-2-phenylindolizin-3-yl and 3-methyl-2-phenylindolizin-1-yl donor and tricyanofuran acceptor end moieties linked by octatetraene π-bridge have been synthesized and systematically characterized by NMR, MS and electronic absorption spectra. The chromophores exhibit absorption in the visible and near IR region. Solvatochromic shifts amounting to ca. 100 nm when passing from dioxane to DMSO solutions are accompanied by appearance of an additional narrow intensive absorption band at ca. 915–950 nm resulting from the cross of cyanine limit and coexistence of two chromophor forms. In low-polar dioxane and chloroform solvents, when one form is manifested, there exists a mixture of *EEEE* and *EEZE*-isomers, while in polar solvents (when two forms are displayed) one isomer is observed resulting from the transformation of configurational isomers into conformers. Small energy gaps of ca. 0.8–0.9 eV between chromophore ground and excited states were determined. For the first time electro-optic activity of indolizine based chromophores was studied: poled film **(MPI-3)-OT-TCF/PMMA** with 10 wt% chromophore load gives r_{33} value of 29 pm/V.

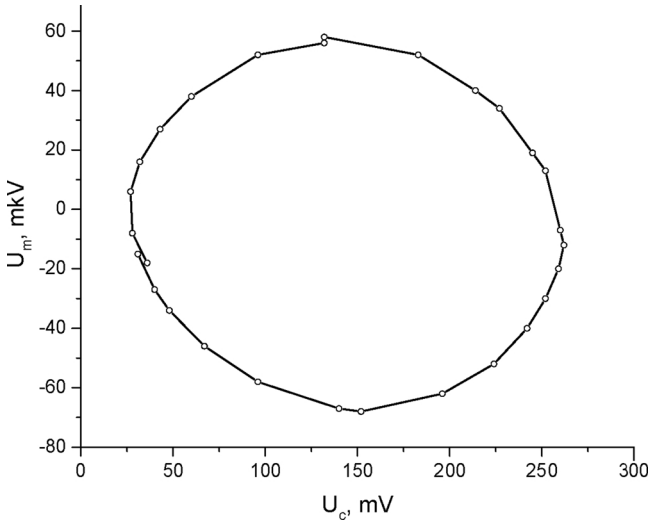

Fig. 9. EO ellipsometric measurement obtained at λ = 1310 nm for θ = 42° for poled **(MPI-3)-OT-TCF/PMMA** film (15 wt%), V_m = 14 V.

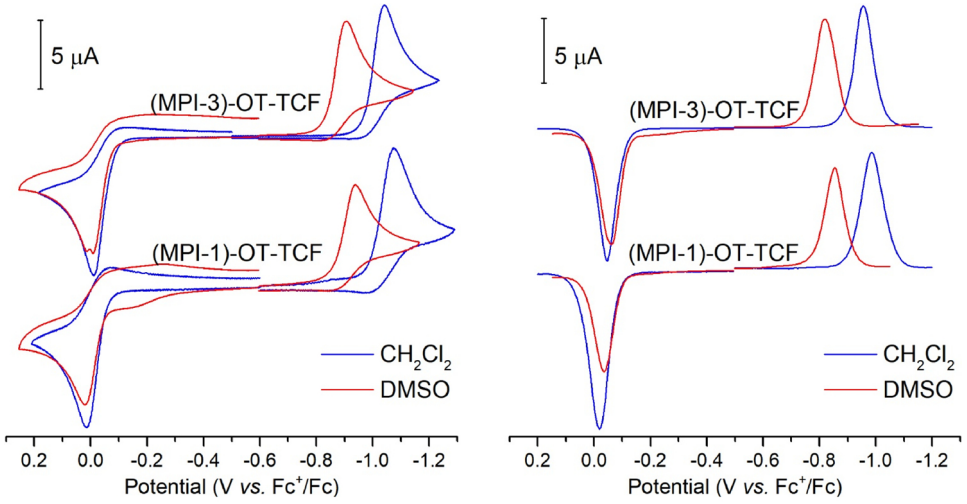

Fig. 8. Cyclic voltammograms of studied chromophores in CH_2Cl_2/0.2 M Bu_4NBF_4 (blue) and DMSO/0.1 M Bu_4NBF_4 (red), scan rate 100 mV/s (a); differential pulse voltammograms of studied chromophores in CH_2Cl_2/0.2 M Bu_4NBF_4 (blue) and DMSO/0.1 M Bu_4NBF_4 (red).

Table 5
EO coefficients of PMMA/**(MPI-3)-OT-TCF.**

Sample	Chromophore content, wt%	Sample drying	T_p, °C	Electrode material	η	r_{33}, pm/V
1	10	At room temperature	119	Ag	0.35	29
2	15	at 60 °C	105	Al	0.18	10
3	15		110	Al	0.27	21
4	15		115	Ag	0.17	22
5	15	At room temperature	119	Ag	0.17	24

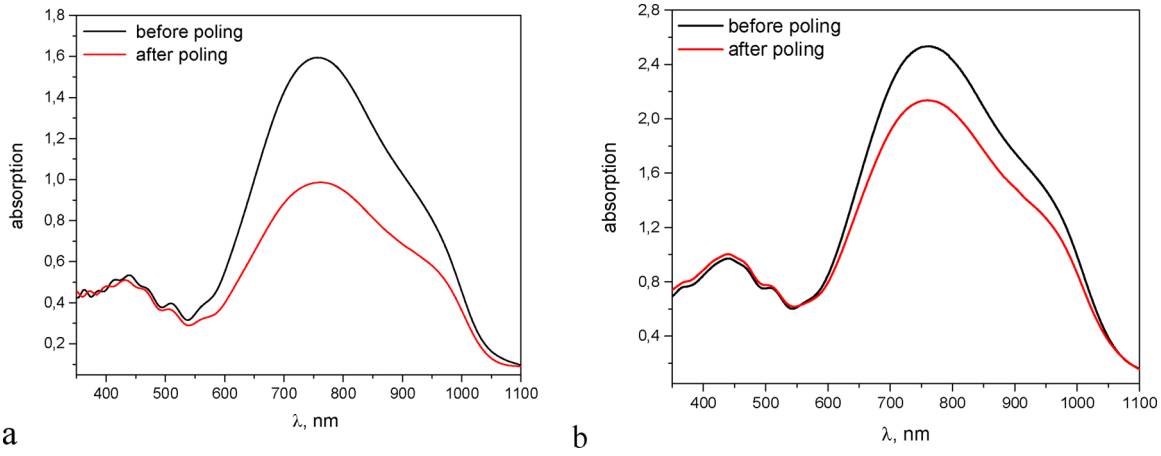

Fig. 10. UV–Vis electronic absorption spectra registered before and after poling for **(MPI-3)-OT- TCF/PMMA** films with chromophore load 10 wt% (a) and 15 wt% (b).

Declaration of Competing Interest

The authors declare no conflict of interest.

Acknowledgment

Financial support of Russian Science Foundation (grant no. 16-13-10215) is gratefully acknowledged.

Appendix A. Supplementary data

Supplementary material related to this article can be found, in the online version, at doi:https://doi.org/10.1016/j.jphotochem.2019.112125.

References

[1] J.A. Davies, A. Elangovan, P.A. Sullivan, B.C. Olbricht, D.H. Bale, T.R. Ewy, C.M. Isborn, B.E. Eichinger, B.H. Robinson, P.J. Reid, X. Li, L.R. Dalton, J. Am. Chem. Soc. 130 (2008) 10565–10575.
[2] M.D.H. Bhuiyan, G.J. Gainsford, Y. Kutuvantavida, J.W. Quilty, A.J. Kay, G.V.M. Williams, M.R. Waterland, Mol. Cryst. Liq. Cryst. 548 (2011) 272–283.
[3] C. Hu, Z. Chen, H. Xiao, Z. Zhen, X. Liu, S. Bo, J. Mater. Chem. C 5 (2017) 5111–5118.
[4] F. Liu, H. Wang, Y. Yang, H. Xu, D. Yang, S. Bo, J. Liu, Z. Zhen, X. Liu, L. Qiu, Dyes Pigm. 114 (2015) 196–203.
[5] J. Wu, C. Peng, H. Xiao, S. Bo, L. Qiu, Z. Zhen, X. Liu, Dyes Pigm. 104 (2014) 15–23.
[6] F. Liu, H. Wang, Y. Yang, H. Xu, M. Zhang, A. Zhang, S. Bo, Z. Zhen, X. Liu, L. Qiu, J. Mater. Chem. C 2 (2014) 7785–7795.
[7] F. Liu, H. Xu, H. Zhang, L. Chen, J. Liu, S. Bo, Z. Zhen, X. Liu, L. Qiu, Dyes Pigm. 134 (2016) 358–367.
[8] X.H. Zhou, J. Luo, J.A. Davies, S. Huang, A.K.Y. Jen, J. Mater. Chem. 22 (2012) 16390–16398.
[9] H. Zhang, F. Huo, F. Liu, Z. Chen, J. Liu, S. Bo, Z. Zhen, L. Qiu, RSC Adv. 6 (2016) 99743–99751.
[10] S.M. Sharipova, A.A. Kalinin, Chem. Heterocycl. Compd. 53 (2017) 36–38 [Khim. Geterotsikl. Soedin. 53 (2017) 36-38].
[11] D.L. Elder, Ch. Haffner, W. Heni, Yu. Fedoryshyn, K.E. Garrett, L.E. Johnson, R.A. Campbell, J.D. Avila, B.H. Robinson, J. Leuthold, L.R. Dalton, Chem. Mater. 29 (2017) 6457–6471.
[12] J. Wu, B. Wu, W. Wang, K.S. Chiang, A.K.-Y. Jen, J. Luo, Mater. Chem. Front. 2 (2018) 901–909.
[13] F. Liu, Sh. Chen, S. Mo, G. Qin, C. Yu, W. Zhang, W.-J. Shi, P. Chen, H. Xu, M. Fu, J. Mater. Chem. C 7 (2019) 8019–8028.
[14] J.H. Yum, P. Walter, S. Huber, D. Rentsch, T. Geiger, F. Nuesch, F. De Angelis, M. Gratzel, M.K. Nazeeruddin, J. Am. Chem. Soc. 129 (2007) 10320–10321.
[15] Y. Hao, X. Yang, J. Cong, H. Tian, A. Hagfeldt, L. Sun, Chem. Commun. (2009) 4031–4033.
[16] H.X. Ji, Z.S. Huang, L. Wang, D. Cao, Dyes Pigm. 159 (2018) 8–17.
[17] R. Chen, X. Yang, H. Tian, L. Sun, J. Photochem. Photobiol. A 189 (2007) 295–300.
[18] Z.S. Wang, N. Koumura, Y. Cui, M. Takahashi, H. Sekiguchi, A. Mori, T. Kubo, A. Furube, K. Hara, Chem. Mater. 20 (2008) 3993–4003.
[19] K. Hara, T. Sato, R. Katoh, A. Furube, Y. Ohga, A. Shinpo, S. Suga, K. Sayama, H. Sugihara, H. Arakawa, J. Phys. Chem. B 107 (2003) 597–606.
[20] C. Shen, Y. Wu, W. Zhang, H. Jiang, H. Zhang, E. Li, B. Chen, X. Duan, W.H. Zhu, Dyes Pigm. 149 (2018) 65–72.
[21] H. Xu, M. Zhang, A. Zhang, G. Deng, P. Si, H. Huang, C. Peng, M. Fu, J. Liu, L. Qiu, Z. Zhen, S. Bo, X. Liu, Dyes Pigm. 102 (2014) 142–149.
[22] X. Zhang, I. Aoki, X. Piao, S. Inoue, H. Tazawa, S. Yokoyama, A. Otomo, Tetrahedron Lett. 51 (2010) 5873–5876.
[23] Y. Yang, J. Liu, H. Xiao, Z. Zhen, S. Bo, Dyes Pigm. 139 (2017) 239–246.
[24] T. Yamada, I. Aoki, H. Miki, C. Yamada, A. Otomo, Mat. Chem. Phys. 139 (2013) 699–705.
[25] S.H. Kim, S.Y. Lee, S.Y. Gwon, Y.A. Son, J.S. Bae, Dyes Pigm. 84 (2010) 169–175.
[26] X. Piao, X. Zhang, S. Inoue, S. Yokoyama, I. Aoki, H. Miki, A. Otomo, H. Tazawa, Org. Electronics 12 (2011) 1093–1097.
[27] A.J. Huckaba, F. Giordano, L.E. McNamara, K.M. Dreux, N.I. Hammer, G.S. Tschumper, S.M. Zakeeruddin, M. Gratzel, M.K. Nazeeruddin, J.H. Delcamp, Adv. Energy Mater. 5 (2015) 1401629.
[28] A.J. Huckaba, A. Yella, L.E. McNamara, A.E. Steen, J.S. Murphy, C.A. Carpenter, G.D. Puneky, N.I. Hammer, M.K. Nazeeruddin, M. Graetzel, J.H. Delcamp, Chem. Eur. J. 22 (2016) 15536–15542.
[29] A.J. Huckaba, A. Yella, P. Brogdon, J.S. Murphy, M.K. Nazeeruddin, M. Graetzel, J.H. Delcamp, Chem. Commun. 52 (2016) 8424–8427.
[30] A.I. Levitskaya, A.A. Kalinin, O.D. Fominykh, I.V. Vasilyev, M.Yu. Balakina, Comp. Theor. Chem. 1094 (2016) 17–22.
[31] A.A. Kalinin, M.A. Smirnov, L.N. Islamova, G.M. Fazleeva, T.A. Vakhonina, A.I. Levitskaya, O.D. Fominykh, N.V. Ivanova, A.R. Khamatgalimov, I.R. Nizameev, M. Yu, Balakina, Dyes Pigm. 147 (2017) 444–454.
[32] J. Gayton, Sh.A. Autry, W. Meador, S.R. Parkin, G.A. Hill Jr, N.I. Hammer, J.H. Delcamp, J. Org. Chem. 84 (2019) 687–697.
[33] J.N. Gayton, Sh. Autry, R.C. Fortenberry, N.I. Hammer, J.H. Delcamp, Molecules 23 (2018) 3051–3062.
[34] Ch.S.L. Rathnamalala, J.N. Gayton, A.L. Dorris, Sh.A. Autry, W. Meador, N.I. Hammer, J.H. Delcamp, C.N. Scott, J. Org. Chem. (2019), https://doi.org/10.1021/acs.joc.9b01860.
[35] J.B. Henry, R.J. MacDonald, H.S. Gibbad, H. McNab, A.R. Mount, Phys. Chem. Chem. Phys. 13 (2011) 5235–5241.
[36] Y. Toya, T. Ochi, Y. Tanabe, M. Nakatsuka, Pat 2009170790 Japan - 2009.

[37] V.A. Mamedov, A.A. Kalinin, A.T. Gubaidullin, S.A. Katsuba, V.V. Syakaev, I.Kh. Rizvanov, Sh.K. Latypov, Tetrahedron 69 (2013) 10675–10687.
[38] V.A. Mamedov, A.A. Kalinin, A.I. Samigullina, E.V. Mironova, D.B. Krivolapov, A.T. Gubaidullin, I.Kh. Rizvanov, Tetrahedron Lett. 54 (2013) 3348–3352.
[39] V.V. Yanilkin, N.V. Nastapova, V.A. Mamedov, A.A. Kalinin, V.P. Gubskaya, Russ. J. Electrochem. 43 (2007) 770–775.
[40] V.V. Yanilkin, N.V. Nastapova, A.S. Stepanov, A.A. Kalinin, V.A. Mamedov, Russ. Chem. Bull. 58 (2009) 89–94.
[41] M.J. Frisch, G.W. Trucks, H.B. Schlegel, G.E. Scuseria, M.A. Robb, J.R. Cheeseman, et al., Gaussian 16, Revision B.01, Gaussian, Inc., Wallingford CT, 2016.
[42] F. Weigend, Phys. Chem. Chem. Phys. 8 (2006) 1057–1065.
[43] F. Weigend, R. Ahlrichs, Phys. Chem. Chem. Phys. 7 (2005) 3297–3305.
[44] T. Yanai, D.P. Tew, N.C. Handy, Cheml. Phys. Lett. 393 (2004) 51–57.
[45] E. Cances, B. Mennucci, J. Tomasi, J. Chem. Phys. 107 (1997) 3032–3041.
[46] J. Tomasi, B. Mennucci, R. Cammi, Chem. Rev. 105 (2005) 2999–3093.
[47] B. Mennucci, E. Cances, J. Tomasi, J. Phys. Chem. B 101 (1997) 10506–10517.
[48] D. Jacquemin, X. Assfeld, J. Preat, E.A. Perpete, Mol. Phys. 105 (2007) 325–331.
[49] J. Preat, P.F. Loos, X. Assfeld, D. Jacquemin, E.A. Perpete, Int. J. Quantum Chem. 107 (2007) 574–585.
[50] R. Bauernschmitt, R. Ahlrichs, Chem. Phys. Lett. 256 (1996) 454–464.
[51] R. Bauernschmitt, M. Haser, O. Treutler, R. Ahlrichs, Chem. Phys. Lett. 264 (1997) 573–578.
[52] F. Furche, J. Chem. Phys. 114 (2001) 5982–5992.
[53] M. Colonna, L. Greci, M. Poloni, J. Chem. Soc. Perkin Trans. 2 (1984) 165–168.
[54] M. Fraser, S. McKenzie, D.H. Reid, J. Chem. Soc. B: Phys. Org. (1966) 44–48.
[55] W.E. Moerner, R.J. Twieg, D.W. Kline, M. He, Pat US 2007:134737.
[56] C. Zhang, L.R. Dalton, M.C. Oh, H. Zhang, W.H. Steier, Chem. Mater. 13 (2001) 3043–3050.
[57] A.A. Kalinin, G.G. Yusupova, T.I. Burganov, Y.B. Dudkina, L.N. Islamova, A.I. Levitskaya, A.R. Khamatgalimov, S.A. Katsyuba, Y.H. Budnikova, M.Yu. Balakina, J. Mol. Struct. 1156 (2018) 74–82.
[58] A.A. Kalinin, G.M. Fazleeva, T.I. Burganov, L.N. Islamova, A.I. Levitskaya, Y.B. Dudkina, G.R. Shaikhutdinova, G.G. Yusupova, M.A. Smirnov, T.A. Vakhonina, N.V. Ivanova, A.R. Khamatgalimov, S.A. Katsyuba, Y.H. Budnikova, I.R. Nizameev, M.Yu. Balakina, J. Photochem. Photobiol. A 364 (2018) 764–772.
[59] F. Liu, H. Xu, H. Zhang, L. Chen, J. Liu, S. Bo, Z. Zhen, X. Liu, L. Qiu, Dyes Pigm. 134 (2016) 358–367.
[60] H. Zhang, F. Huo, F. Liu, Z. Chen, J. Liu, S. Bo, Z. Zhen, L. Qiu, RSC Adv. 6 (2016) 99743–99751.
[61] F. Liu, H. Wang, Y. Yang, H. Xu, M. Zhang, A. Zhang, S. Bo, Z. Zhen, X. Liu, L. Qiu, Mater. Chem. 2 (2014) 7785–7795.
[62] Y. Yang, J. Liu, H. Xiao, Z. Zhen, S. Bo, Dyes Pigm. 139 (2017) 239–246.
[63] A.A. Kalinin, S.M. Sharipova, T.I. Burganov, Yu.B. Dudkina, A.R. Khamatgalimov, S.A. Katsyuba, Yu.H. Budnikova, M.Yu. Balakina, Dyes Pigm. 146 (2017) 82–91.
[64] A.A. Kalinin, S.M. Sharipova, T.I. Burganov, A.I. Levitskaya, O.D. Fominykh, T.A. Vakhonina, N.V. Ivanova, A.R. Khamatgalimov, S.A. Katsyuba, M.Yu. Balakina, J. Photochem. Photobiology A. 370 (2019) 58–66.
[65] P.A. Bouit, C. Aronica, L. Toupet, B. Le Guennic, C. Andraud, O. Maury, J. Am. Chem. Soc. 132 (2010) 4328–4335.
[66] R.S. Lepkowicz, O.V. Przhonska, J.M. Hales, J. Fu, D.J. Hagan, E.W. Van Stryland, M.V. Bondar, Yu.L. Slominsky, A.D. Kachkovski, Chem. Phys. 305 (2004) 259–270.
[67] M. He, T.M. Leslie, J.A. Sinicropi, S.M. Garner, L.D. Reed, Chem. Mater. 14 (2002) 4669–4675.
[68] T.I. Burganov, S.A. Katsyuba, S.M. Sharipova, A.A. Kalinin, A. Monari, X. Assfeld, Phys. Chem. Chem. Phys. 20 (2018) 21515–21527.
[69] T.I. Burganov, N.A. Zhukova, V.A. Mamedov, C. Bannwarth, S. Grimme, S.A. Katsyuba, Phys. Chem. Chem. Phys. 19 (2017) 6095–6104.
[70] T.I. Burganov, S.A. Katsyuba, T.A. Vakhonina, A.V. Sharipova, O.D. Fominykh, M.Yu. Balakina, J. Phys. Chem. C 122 (2018) 1779–1785.
[71] C. Adamo, G.E. Scuseria, V. Barone, J. Chem. Phys. 111 (1999) 2889–2899.
[72] C. Adamo, V. Barone, J. Chem. Phys. 110 (1999) 6158–6170.
[73] T. Yanai, D.P. Tew, N.C. Handy, Chem. Phys. Lett. 393 (2004) 51–57.
[74] T.I. Burganov, S.A. Katsyuba, L.N. Islamova, G.M. Fazleeva, S.M. Sharipova, A.A. Kalinin, A. Monari, X. Assfeld, Dyes Pigm. 170 (2019) 107580.
[75] B. Mennucci, E. Cances, J. Tomasi, J. Phys. Chem. B 101 (1997) 10506–10517.
[76] D. Jacquemin, X. Assfeld, J. Preat, E.A. Perpete, Mol. Phys. 105 (2007) 325–331.
[77] J. Preat, P.F. Loos, X. Assfeld, D. Jacquemin, E.A. Perpete, Int. J. Quantum Chem. 107 (2007) 574–585.
[78] M.Yu. Balakina, J. Li, V.M. Geskin, S.R. Marder, J.L. Bredas, J. Chem. Phys. 113 (2000) 9598–9609.
[79] C.M. Cardona, W. Li, A.E. Kaifer, D. Stockdale, G.C. Bazan, Adv. Mater. 23 (2011) 2367–2371.
[80] O.K. Kim, A. Fort, M. Barzoukas, M. Blanchard-Desce, J.M. Lehn, J. Mater. Chem. 9 (1999) 2227–2232.
[81] C.C. Teng, H.T. Man, Appl. Phys. Lett. 56 (1990) 1734–1736.
[82] Y. Shuto, M. Amano, J. Appl. Phys. 77 (1995) 4632–4638.